DISSERTATION

EXPLORING PRECIPITATION PROCESSES IN STRATOCUMULUS CLOUDS FROM SATELLITE-DERIVED CLOUD PROPERTIES

Submitted by

Yasutaka Murakami

Department of Atmospheric Science

In partial fulfillment of the requirements

For the Degree of Doctor of Philosophy

Colorado State University

Fort Collins, Colorado

Fall 2021

Doctoral Committee:

Advisor: Christian D. Kummerow
Co-Advisor: Susan C. van den Heever

Christine Chiu
Chandrasekaran

ABSTRACT

EXPLORING PRECIPITATION PROCESSES IN STRATOCUMULUS CLOUDS FROM SATELLITE-DERIVED CLOUD PROPERTIES

Marine stratocumulus clouds are low-level convective clouds that develop within the marine atmospheric boundary layer and have a large impact on the global radiation budget and hydrological cycle. Drizzle plays an important but complicated role in their longevity and microphysical properties. Many studies have examined the response of cloud base rain rate to varying cloud droplet number concentrations and cloud thickness, as well as liquid water path (LWP), and found that cloud base rain rates are enhanced with lower cloud droplet number concentrations and greater cloud thickness or LWP.

In warm stratocumulus clouds, cloud base rain rate is a combination of raindrop embryo production through collision coalescence (i.e. autoconversion) and raindrop embryo growth by collecting cloud droplets (i.e. accretion). Previous studies have shown that cloud base rain rate depends on LWP or cloud thickness and the geographical location of stratocumulus clouds, but the dependence of the autoconversion process on these variables is not well known because cloud base rain rate represents the effects of both autoconversion and accretion. This two-part dissertation explores the dependence of stratocumulus cloud precipitation processes on cloud thickness and geographical location by examining the cloud properties retrieved by A-Train satellite observations from *CloudSat's* Cloud Profiling Radar (CPR), CALIPSO's Cloud-Aerosol Lidar with Orthogonal Polarization (CALIOP) and Aqua's Moderate Resolution Imaging Spectroradiometer (MODIS).

In the first part, the relations between cloud top properties (radar reflectivity, LWC and cloud droplet number concentration) and cloud geometrical thickness are investigated for subtropical stratocumulus clouds. Satellite-observations show that cloud top LWC and effective

radius increase as clouds become thicker. The data also suggest that autoconversion may be more efficient in thicker clouds. These findings are consistent with previous studies that have shown that thicker clouds have larger cloud droplets and thus produce more rain embryos. However, it is also found that clouds separate into two sub-groups as they transition from thick (i.e. geometrical thickness of 384-480m) to very thick clouds (i.e. geometrical thickness of 624-720m). Drizzling clouds have higher LWC and their drops have larger effective radii, whereas non-drizzling clouds have lower cloud top LWC and smaller effective radii.

In the second part, the climatology of satellite-derived cloud top properties (radar reflectivity, LWC and cloud droplet number concentration) for 8 stratocumulus cloud regions are presented. While LWP tends to be larger for midlatitude clouds, cloud top LWC tends to be larger at subtropical stratocumulus clouds. Since midlatitude stratocumulus clouds are thicker, these results suggests that effective condensation rates are larger for subtropical stratocumulus clouds. Both cloud top and cloud base radar reflectivity also tend to be larger for subtropical stratocumulus clouds. Based on these findings, the sensitivity of cloud top radar reflectivity on LWC and cloud droplet number concentration are examined. Cloud top radar reflectivity is more (less) sensitive to changes in LWC and cloud droplet number concentration for clouds with stronger (weaker) cloud top radar reflectivity. This is consistent with previous findings that collision-coalescence efficiency between liquid water droplets (i.e. approximately 20 μm in diameter) increases non-linearly with droplet size.

The overall results presented in this dissertation indicate that the autoconversion process can be represented with a globally applicable function of cloud top LWC and cloud droplet number concentration for all stratocumulus clouds regardless of their geolocation and geometrical thickness. It is also demonstrated that cloud top raindrop embryo generation rate is an important factor for determining the precipitation generation rate for stratocumulus clouds as a whole. In general, accretional growth is controlled by both the total cross-sectional area of rain drops and LWP. By comparing spatial patterns of cloud top radar reflectivity (i.e. total cross-sectional area of rain drops) and radar reflectivity increase from cloud top to bottom (i.e. accretional growth), it

is found that accretional growth depends more on total cross-sectional area of rain drops and less on LWP in stratocumulus clouds.

These conclusions can explain the findings of previous studies that cloud base rain rate depends on LWP (or cloud thickness) and geographical location of stratocumulus clouds. Cloud base rain rate is dependent on geometrical thickness because cloud top LWC increases as cloud become thicker. Subtropical stratocumulus clouds tend to have stronger precipitation at a given LWP compared to midlatitude stratocumulus clouds because the effective condensation rate of subtropical stratocumulus clouds is greater and so is the cloud top LWC. In this study, the effect of Cloud Condensation Nuclei on warm rain processes is represented by varying cloud droplet number concentration. The results presented in this dissertation represent more than one hundred thousand independent pixels and provide a statistically robust benchmark that numerical models should reproduce.

ACKNOWLEDGEMENTS

I would like to thank Prof. Christian Kummerow and Prof. Susan van den Heever for their mentorship and guidance throughout the completion of my graduate program. I would also like to thank the committee members of my doctoral committee, Prof. Christine Chiu and Prof. Chandrasekaran Venkatachalam, for their time and suggestions to my research.

I am also grateful to the staff member of the CloudSat Data Processing Center, which is run by Cooperative Institute for Research in the Atmosphere, for their technical assistance to utilize the data. This research was supported by the Japanese Government Long-term Overseas Fellowship Program.

TABLE OF CONTENTS

Chapter 1

Introduction

1.1 Stratocumulus clouds

Marine stratocumulus clouds are low-level convective clouds that develop within the marine atmospheric boundary layer. Due to their relatively low cloud top height, stratocumulus clouds have negative radiative forcing because they reflect much of the incoming solar radiation but have little effect on the outgoing longwave radiation. They cover wide areas of Earth's ocean surface and have a significant impact on the global radiation budget and hydrological cycle (Slingo 1990). On an annual average, they cover approximately one-fifth of global ocean surface (Wood 2012).

Stratocumulus are likely to be found within the marine boundary layer formed in the subsiding regions of large-scale weather system such as the Hadley and Walker Circulation in the subtropics (e.g. Klein and Hartmann 1993), baroclinic storm systems (e.g. Norris and Klein 2000) and cold-air outbreaks (e.g. Klein and Hartmann 1993) in the mid-latitudes. Subtropical oceans off the western coast of Americas and Africa are especially susceptible to persistent warm stratocumulus clouds, which makes these regions favorable for studying cloud physical processes of warm rain clouds. In these regions, a strong inversion layer is formed by the subsidence from the subtropical high and low sea surface temperature due to cold currents and coastal upwelling.

1.2 Drizzle

Marine stratocumulus clouds are often associated with drizzle. Drizzle has an impact on the longevity and microphysical properties of stratocumulus clouds by modulating the microphysical structure of stratocumulus clouds as well as the thermodynamical structure of stratocumulus-topped marine boundary layer by redistributing heat and water vapor (Wood 2012). To better understand the life cycle of these stratocumulus clouds, it is therefore imperative that their precipitation processes to be better understood.

In warm stratocumulus clouds, rain embryos are generated by collision-coalescence among

cloud droplets. The collision-coalescence kernel is a strong function of droplet size. Following Long (1974), collision-coalescence kernel is proportional to the sixth power of collector drop radius for collision-coalescence among cloud droplets. The mass increase of collector cloud droplets by collision-coalescence is proportional to the product of collected droplet mass and collision-coalescence efficiency. Thus, rain embryo generation is maximized when cloud liquid water content (LWC) and cloud droplet size are the largest.

In-situ observations show that cloud LWC and cloud droplet size increase upward within the stratocumulus clouds and their largest values are found near the cloud top (e.g. Nicholls and Leighton 1986; Wood 2005a). Wood (2005b) calculated the rain embryo production rate by applying a stochastic collection equation to droplet size distribution obtained from aircraft in-situ measurement of stratocumulus clouds. They showed that rain embryos are mostly produced near the cloud top. Once raindrop embryos are generated near the cloud top, they grow by collecting cloud droplets while falling through cloud layer and then gradually evaporate at sub-cloud layer.

Precipitation processes in stratocumulus clouds have been extensively studied from the viewpoint of the impact of changing background aerosol serving as Cloud Condensation Nuclei (CCN) on precipitation efficiency, the spatial distribution and lifetime of cloud systems. This impacts is commonly referred to as the second aerosol indirect effect (Albrecht 1989). Since cloud droplet number concentrations generally increase with increasing number concentrations of aerosol particles that act as CCN (Twomey 1959), many observational and numerical simulation studies have examined the response of cloud base rain rate to varying cloud droplet number concertation. While the impact of varying CCN concentration on the longevity of stratocumulus clouds differs by studies, most observational and modelling studies have found that higher cloud droplet number concentrations suppress cloud base rain rate. Many field campaigns conducted in the southeast Pacific (e.g. Comstock et al. 2004; Wood et al. 2011), northeast Pacific (e.g. van Zanten et al. 2005; Lu et al. 2007,2009), and northeast Atlantic (e.g. Wood 2005a; Mann et al. 2014) have shown that cloud base rain rate in stratocumulus clouds is suppressed by higher cloud droplet number concentrations. Leon et al. (2008) found similar trends from A-train satellite

observations. Various modeling studies, including those utilizing Large-eddy-simulation (LES; e.g. Ackerman et al. 2003) and cloud resolving model simulation（e.g. Wang et al. 2011), also suggest that cloud base rain rates of stratocumulus clouds decrease with higher cloud droplet number concentration. They also found that intensity of cloud base rain rate not only decreases with increasing cloud droplet number concentration but also intensifies with increasing LWP or cloud thickness (H). Several empirical relations have been proposed to represent cloud base rain rate as a power-law of LWP or H and cloud droplet number concentration based on observations (e.g., Comstock et al., 2004; Vanzanten et al., 2005).

Cloud base rain rate in stratocumulus clouds has been found to depend not only on cloud geometrical thickness but also on their geographical location. Leon et al. (2008) investigated the global characteristic of marine stratocumulus cloud precipitation by utilizing space-borne observation from the A-Train satellites. They found that the cloud base rain rate of marine stratocumulus clouds is weaker in midlatitude regions compared to that of subtropical regions. Their results also showed the relatively simple dependence of cloud base rain rate on LWP and cloud droplet effective radius (r_e). The relation among these variables appeared to be different between midlatitude and subtropical regions where subtropical stratocumulus clouds tends to have larger cloud base rain rates. Likewise, their dependence of drizzle occurrence on LWP and r_e showed similar relations for both subtropical and midlatitude stratocumulus clouds, but drizzle occurrence was more sensitive to LWP in subtropics.

1.3 Bulk microphysical representation of drizzle formation processes

While rain embryo generation through collision-coalescence among cloud droplets and raindrop growth by collecting cloud droplets are a continuous phenomenon, most bulk microphysics schemes utilized in numerical weather prediction models discretize the process into two categories: autoconversion and accretion. Autoconversion represents the conversion of cloud droplets to raindrop embryos through collision-coalescence among cloud droplets. Accretion represents the growth of rain drops by collecting cloud droplets. In this dissertation, we will

distinguish these two processes following the treatment of bulk microphysics representation.

Autoconversion and accretion rate are primally determined by the droplet size distribution and collision-coalescence efficiency. Many bulk parameterizations have been proposed with different assumptions on droplet size distributions and collision-coalescence efficiencies (e.g. Berry and Reinhardt 1974; Khairoutdinov and Kogan 2000), which express autoconversion and accretion as a power law of LWC and cloud droplet number concentration (Liu and Daum 2004). In these schemes, cloud top raindrop embryo production (i.e. autoconversion) increases with lager LWC and smaller cloud droplet number concentration, which is consistent with the fact that collision-coalescence efficiency increases with droplet size.

1.4 Motivation

In many previous observational studies, LWP and cloud droplet number concentration were the key variables examined to understand cloud base rain rates (e.g. Wood 2005a; Vanzanten et al. 2005). These studies showed that LWP increases with cloud geometrical thickness. They also showed that cloud base rain rate is dependent on cloud geometrical thickness and geographical location (e.g. Comstock et al. 2004; Leon et al. 2008), which means that the sum of autoconversion and accretion differ by cloud geometrical thickness and their geographical location. However, it has been difficult to obtain insight for each separate process because cloud base rain rate contains information on both autoconversion and accretion.

Also, utilization of LWP instead of LWC makes it difficult to obtain insights into the dependence of autoconversion on cloud geometrical thickness and geographical location because autoconversion is modulated by LWC and not by LWP. While observations (e.g. Wood 2005a) show that LWC increases linearly within cloud layers, in general, cloud top LWC is not merely a function of cloud geometrical thickens because effective condensation rates vary with clouds. Brenguier et al. (2011) found from in-situ observation form the Dynamics and Chemistry of Marine Stratocumulus cloud experiment (DYCOM-II) that adiabaticity (ratio of actual condensation rate to adiabatic condensation rate) of stratocumulus clouds in the southeastern

Pacific Ocean varies from 0.67 to 0.90. Adiabatic condensation rates and evaporation due to cloud top entrainment varies with clouds depending on their environment. Strictly speaking, cloud droplet number concentrations are also not vertically constant as assumed in these studies. Cloud droplet number concentration fluctuates within cloud layers due to many factors. For example, evaporation of cloud droplets by dry air entrainment and collision-coalescence among cloud droplets tend to lower the cloud droplet number concentration at cloud top as clouds become thicker.

In order to better understand the dependence of autoconversion and accretion on cloud thickness and geographical location, this dissertation investigates the cloud properties of stratocumulus clouds retrieved from A-Train satellites with a focus on cloud top properties. Examining the dependence of cloud top radar reflectivity, cloud droplet number concentration and LWC on cloud thickness and geographical location allow us to discuss the autoconversion in a more physically sound and straightforward manner. While often limited in their spatial resolution, satellite observations have the advantage over ground-based observations in their ability to obtain vast amounts of data to draw statistically robust results over many distinct regions, as well as observing cloud top liquid hydrometeors without having to address the effects of rain and water vapor attenuation.

1.5 Outline of dissertation

This dissertation consists of two parts, both of which examine autoconversion and accretion processes in stratocumulus clouds from satellite-derived cloud properties. The organization of this dissertation is as follows. The data and methodology used to estimate cloud properties from A-Train satellite observations is described in Chapter2. Chapter 3 investigates the dependence of cloud properties of subtropical stratocumulus clouds on cloud geometrical thickness and discusses the implications for precipitation processes. Chapter 4 investigates the difference of cloud properties between subtropical and midlatitude stratocumulus clouds and again discusses the implications for precipitation processes and previous findings. The key findings of the dissertation

are summarized in Chapter 5.

Chapter 2
Data and methods

2.1 Analyzed stratocumulus clouds

Cloud parameters of warm stratocumulus clouds are estimated from A-Train satellite observations. This includes *CloudSat*'s Cloud Profiling Radar (CPR) (Stephens et al. 2002), CALIPSO's Cloud-Aerosol Lidar with Orthogonal Polarization (CALIOP) (Winker et al. 2009) and Aqua's Moderate Resolution Imaging Spectroradiometer (MODIS) (Parkinson 2003). All data are matched up to *CloudSat* footprints. The horizontal and vertical resolutions of *CloudSat* observations are approximately 1.75km and 240m, respectively. CALIOP observations have a horizontal resolution of 333m and vertical resolution of 30-60m depending on the altitude.

In this study, warm stratocumulus clouds are defined as single-layer low-level clouds whose cloud top height and temperature are below 3000m and above 268K, respectively. Cloud layer information is obtained from the 2B-GEOPROF-LIDAR product (Mace and Zhang 2014), which is a merged product derived from *CloudSat* radar reflectivity and CALIOP lidar backscatter profiles. Cloud top height is obtained from the CAL_LID_L2_01kmCLay product which provides cloud top height based on CALIOP lidar backscatter profile. Cloud top temperature is obtained from the ECMWF-AUX product which is a set of state variables of the fifth generation ECMWF reanalysis (ERA5) interpolated to each *CloudSat* bin.

The definition of stratocumulus clouds follows that of the International Satellite Cloud Climatology Project (ISCCP; Rossow and Schiffer 1991), which defines low clouds as clouds with top pressures of more than 680hPa, or maximum cloud top geometric heights of 3000m corresponding to 680 hPa in pressure coordinates. Following a previous study focused on estimating cloud droplet number concentration of stratocumulus clouds (Bennartz and Rausch 2017), the minimum cloud top temperature is set to 268K in order to focus on warm clouds. Three years of data from 2008 to 2010 are analyzed. While A-Train satellites have day and night observations, only daytime observations (around 13:30 local time) are analyzed because MODIS

optical thickness and cloud droplet effective radius, which need visible reflectance, are utilized for estimating cloud properties.

The definition of the analysis regions follows Muhlbauer et al. (2014) which investigated the climatology of stratocumulus clouds using A-Train observations. In Chapter 3, stratocumulus clouds from three subtropical regions, namely Northeast Pacific (NEP), Southeast Pacific (SEP) and Southeast Atlantic (SEA) are analyzed to examine the dependence of cloud top properties on cloud geometrical thickness. Table 2.1 defines the three regions analyzed in Chapter 3, as well as the number of pixels that passed quality control procedures in each region. Figure 2.1 shows the global distribution of occurrence of clouds defined as stratocumulus clouds that passed the quality control procedure described below. Regions enclosed by the red lines are the three analysis domains in Chapter 3. It is clear that the three analysis regions focused in Chapter 3 have a greater chance of observing stratocumulus clouds satisfying the criteria in this study.

In Chapter 4, eight stratocumulus clouds regions in the subtropics and midlatitude are chosen for examining the difference between midlatitude and subtropical stratocumulus clouds. Table 2.2 shows the details of the study regions. Except for the Southern Ocean, each region has similar areal extent. Subtropical regions have larger data counts compared to the midlatitude regions except for Southern Ocean and Northeast Atlantic. This is partially due to fact that we are selecting only warm stratocumulus clouds. While midlatitude stratocumulus clouds consist of both warm and mix-phased clouds, subtropical stratocumulus clouds are dominated by warm clouds.

2.2 Cloud properties

2.2.1 Cloud top LWC and cloud droplet number concentration

Cloud top LWC and cloud droplet number concentration are derived from CALIOP layer-integrated depolarization ratio from the LID_L2_05kmCPro product and MODIS effective radius from the MOD06-1KM-AUX product which is a subset of MODIS Collection 6 data (Platnick et al. 2017) matched to the closest *CloudSat* footprints. Following Hu et al. (2007), cloud top LWC and cloud droplet number concentrations are computed as:

$$LWC = \frac{0.002 r_e}{3}\left(\frac{r_e}{1\mu m}\right)^{\frac{1}{3}}\left\{1 + 135\frac{\delta^2}{(1-\delta)^2}\right\} \quad (2.1)$$

$$N_d = 1000\frac{1 + \frac{135\delta^2}{(1-\delta)^2}}{2\pi\left(\frac{r_e}{1\mu m}\right)^{5/3}} \quad (2.2)$$

where LWC is in gm^{-3}, $N_d(cm^{-3})$ is cloud droplet number concentration, $r_e(\mu m)$ is the MODIS 3.7 μm cloud droplet effective radius and δ is unitless layer-integrated depolarization ratio. Hu et al. (2007) derived the empirical relations of layer-integrated depolarization, extinction coefficient and effective radius from Monte Carlo simulations of clouds. CALIOP backscatter is a lidar signal scattered by cloud droplets near cloud top in the case of stratocumulus clouds. Lidar backscatter becomes more depolarized with increasing multiple scattering, which means that clouds with denser cloud droplet number concentrations show larger depolarization ratios. Unlike MODIS-derived cloud parameters, the method does not make assumptions about the vertical profile of stratocumulus clouds.

2.2.2 Cloud geometrical thickness

Cloud geometrical thickness is defined as the height difference between cloud top and base. Cloud top height is determined by CALIOP lidar backscatter profiles and obtained from the CAL_LID_L2_01kmCLay product. Cloud base height is determined by radar reflectivity profiles from the 2B-GEOPROF product (Marchand et al. 2008) and defined as the altitude of the bottom of the radar bin with the largest reflectivity among the bins between the fifth bin from the surface (i.e. 960m from the surface) and cloud top height identified by CAL_LID_L2_01kmCLay product. As shown in previous observational studies (Wood 2005a; vanZanten et al. 2005), stratocumulus clouds have their radar reflectivity maximum around cloud base. In stratocumulus clouds, rain drops grow while falling through the cloud layer by collecting cloud droplets but they tend to shrink in the sub-cloud layer due to evaporation. The nearest 4 bins to the surface (i.e. below 960m in altitude) are excluded from the analysis because these bins are heavily contaminated by surface clutter (Marchand et al. 2008). While excluding the nearest 4 bins to the surface might lead to the

overestimation of cloud base height for clouds with actual base heights below 1km, it seems that the treatment has little impact on estimating cloud geometrical thickness because the results agree with that of Wood and Bretherton (2004) who estimated cloud geometrical thickness from MODIS observation. Assuming linear increases of LWC within the cloud layer, they estimated the cloud geometrical thickness by combining adiabatic condensation rate based on MODIS cloud top temperature and pressure with MODIS estimate of LWP.

Figure 2.2 shows the probability density distribution of cloud geometrical thickness defined in this study for SEP, NEP, SEA and all three subtropical stratocumulus area (SUBS), which has a mode located around 200-300m.

2.2.3 Cloud top and base radar reflectivity

CloudSat operates at a frequency of 94GHz which is heavily attenuated by water vapor and hydrometeors. Water vapor attenuation is corrected with the value provided in the 2B-GEOPROF product. Cloud droplet attenuation (dB/km) is calculated as $LWC \cdot \mathrm{a}\theta^b$, which is adopted from Liebe et al. (1989). *LWC* is in gm^{-3}, θ is defined as

$$\theta = {}^{300}/_{T_{cb}} \tag{2.3}$$

where $T_{cb}(K)$ is cloud base air temperature, $a = 3.73$ and $\mathrm{b} = 2.81$.

Figure 2.3 shows the probability density distribution of cloud base and top radar reflectivity as a function of cloud geometrical thickness for three subtropical stratocumulus region analyzed in Chapter 3 (i.e. SEP, NEP, SEA). Vertical gray lines indicates where the top of the *CloudSat* bin matches with the cloud top determined by CALIOP backscatter profile. The cloud top radar reflectivity shows a 240 meter periodic fluctuation especially in regions with radar reflectivity exceeding -20dBZ. Cloud top radar reflectivity increases as a greater proportion of the cloud top radar bin is filled with clouds.

Cloud top radar reflectivity is heavily influenced by the magnitude of vertical partial beam filling effect caused by the fairly coarse vertical resolution of *CloudSat* (240m). It can, however,

be corrected using CALIOP (30m) cloud top information. In this study, the vertical partial beam filling effect is called as the vertical cloud fill ratio and quantified as follows:

$$\text{Vertical cloud fill ratio } = \frac{\mathrm{h(ct)} - \mathrm{h(ctbin\_b)}}{240} \tag{2.4}$$

where 240 represent the geometrical thickness of *CloudSat* radar bin in meters; $\mathrm{h(ct)}$ and $\mathrm{h(ctbin\_b)}$ in Eq. (2.4) denote geometrical height in meters for cloud top determined by CALIOP and the bottom of cloud top radar bin, respectively. In order to reduce the vertical partial beam filling effect, analysis is limited to observations whose vertical cloud fill ratio exceeds 0.6. The white stripes in Figure 2.2 denote clouds whose vertical cloud fill ratio exceeds 0.6.

Clouds are categorized into three groups by their cloud geometrical thickness. In this study, clouds with geometrical thickness of 144-240m (i.e., clouds exist in one *CloudSat* bin), 384-480m (i.e., clouds extend over two *CloudSat* bin) and 624-720m (i.e., clouds extend over three *CloudSat* bin) are analyzed and are hereafter referred as average, thick and very thick clouds, respectively. Table 2.3 shows the data count for each cloud group with different geometrical thickness for the three subtropical stratocumulus regions analyzed in Chapter 3 (i.e. SEP, NEP, SEA). Screening clouds with their vertical cloud fill ratio reduces the samples by approximately 60%.

In contrast to cloud top radar reflectivity, cloud base radar reflectivity tends to continuously increase as cloud become thicker, which agrees with previous studies that have found that cloud base rain rate increases with cloud geometrical thickness. In drizzling clouds, drizzle drops are the major contributor to radar reflectivity. The vertical partial beam filling effect has only a small influence on cloud base radar reflectivity because drizzle drops evaporate gradually below the cloud layer and thus the vertical change of radar reflectivity is also gradual.

2.2.4 LWP

Assuming a cloud model in which LWC increase linearly within the cloud layer, LWP can be computed as (Miller et al. 2016):

$$LWP = \frac{5}{9}\rho_w \tau\, r_e \tag{2.5}$$

where $\rho_w(kgm^{-3})$ is the density of water, τ is the unitless cloud optical thickness and $r_e(\mu m)$ is the cloud droplet effective radius inferred from $3.7\mu m$ ($r_{e,3.7}$). Optical depth and effective radius are obtained from the MOD06-1KM-AUX product. While the MODIS cloud product provides effective radius estimates using observations from $1.6\mu m$, $2.1\mu m$ and $3.7\mu m$, $r_{e,3.7}$ is utilized because it is less prone to pixel heterogeneity compared to the other two. Following Grosvenor et al. (2018), LWP calculation is limited to those pixels satisfy $\tau > 5$ and $r_{e,3.7} > r_{e,2.1} > r_{e,1.6}$. Since the penetration depth of photons at $1.6\mu m$ is deeper than that at $3.7\mu m$, the ordering of retrieved effective radius at various wavelengths satisfies the cloud model assumed in Eq.(2.5). Optically thin clouds are removed because they typically have larger estimation errors for their retrieved cloud properties.

Table 2.1 Stratocumulus domains in subtropical regions and their data counts.

Region	Domain	Data Count
Northeast Pacific(NEP)	15-35N, 120-140W	5.9×10^4
Southeast Pacific(SEP)	10-30S, 75-95W	8.5×10^4
Southeast Atlantic(SEA)	10-30S, 10W-10E	6.7×10^4

Table 2.2 Stratocumulus domains in global studies and their data count.

Region	Domain	Data Count
Northeast Pacific(NEP)	15-35N, 120-140W	1.9×10^4
Southeast Pacific(SEP)	10-30S, 75-95W	3.3×10^4
Northeast Atlantic(NEA)	10-30N, 25-45W	3.9×10^3
Southeast Atlantic(SEA)	10-30S, 10W-10E	2.5×10^4
Southeast Indian Ocean(SEI)	20-40S, 90-110E	1.2×10^4
North Pacific(NP)	40-60N, 165-185E	7.3×10^3
North Atlantic(NA)	45-65N,30-50W	6.8×10^3
Southern Ocean(SO)	45-65S, 180W-180E	5.7×10^4

Table 2.3 Data counts for clouds with different geometrical thickness for the three subtropical stratocumulus domains (i.e., SEP,SEA,NEP).

Cloud Thickness (m)	**Data Count**
144-240 (average)	5.0×10^4
384-488 (thick)	2.5×10^4
624-720 (very thick)	3.4×10^3
All	2.0×10^5

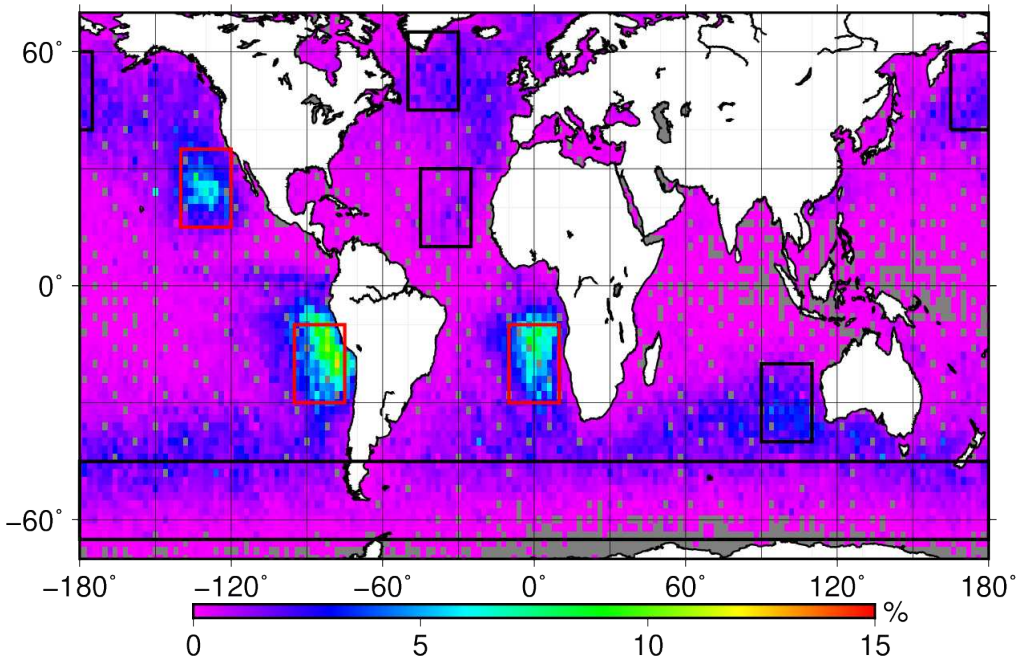

Figure 2.1 Frequency of occurrence of low clouds observed by CloudSat/CALIPSO for those defined as stratocumulus clouds and passing quality controls in this study. Regions enclosed by red rectangles indicates the analysis areas in Chapter 3. Regions enclosed by red and black rectangles indicates the analysis areas in Chapter 4.

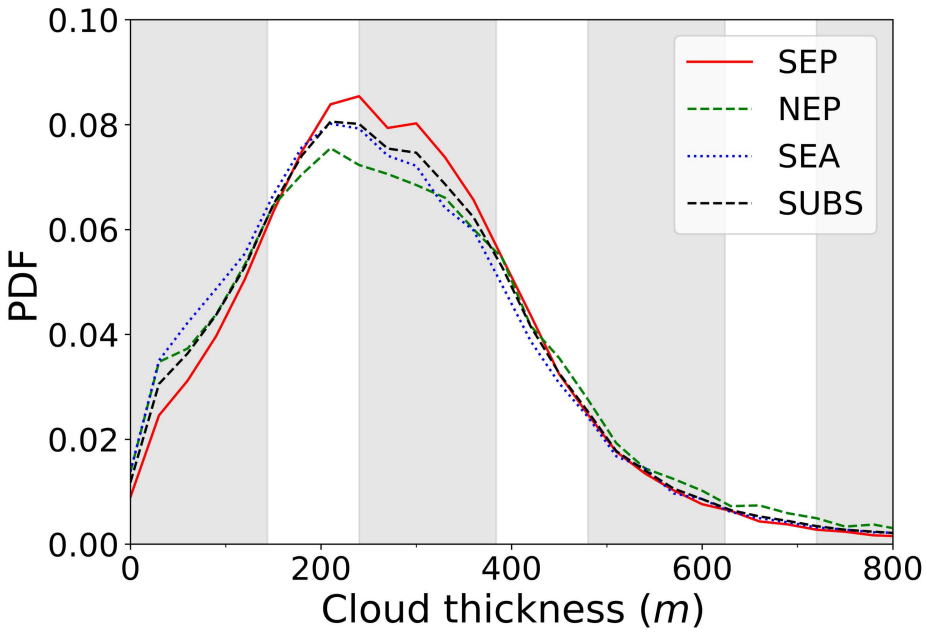

Figure 2.2 Probability density distribution of cloud geometrical thickness for Southeast Pacific(SEP), Northeast Pacific(NEP), Southeast Atlantic(NEA) and all three subtropical stratocumulus area (SUBS). White blank areas denote clouds with whose cloud top *CloudSat* bin satisfies vertical cloud fill > 0.6. Bin size is 30m.

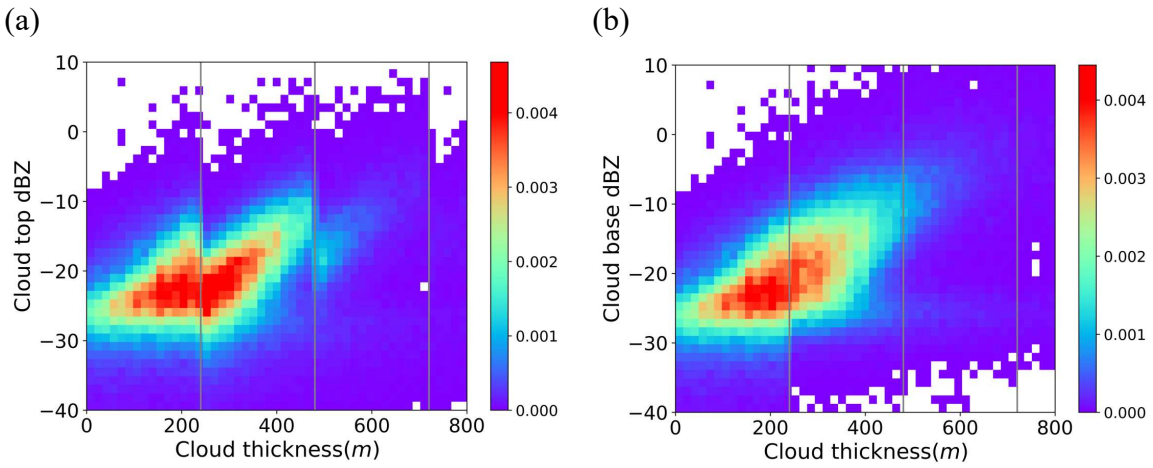

Figure 2.3 Probability density distribution of radar reflectivity as a function of cloud geometrical thickness for (a) cloud base and (b) cloud top.

Chapter 3

Dependency of cloud top properties on cloud geometrical thickness and their implications to precipitation processes in subtropical stratocumulus clouds

3.1 Relations between cloud top properties and cloud geometrical thickness

Figure 3.1 shows the probability density function (PDF) of cloud top and base radar reflectivity, cloud top LWC, LWP, effective radius and near cloud top cloud droplet number concentration, respectively. The PDFs of most of these parameters show distinct behaviors as clouds transition from average to thick and from thick to very thick.

Cloud top radar reflectivity tends to become larger as clouds transition from average to thick clouds (Fig. 3.1a). While the PDFs of cloud top radar reflectivity for average and thick clouds show a unimodal distribution, that of very thick clouds shows a distinct bimodal distribution. The two modes of the PDF are both larger and smaller than that of the average clouds. Cloud top (Fig. 3.1a) and cloud base (Fig. 3.1b) radar reflectivity have similar PDFs for each cloud geometrical thickness. In thick clouds, relatively high radar reflectivity (i.e. more than approximately -10dBZ) is more frequent at cloud base compared to cloud top. While the PDFs of both cloud top and base radar reflectivity have a mode located around -25dBZ in very thick clouds, the higher mode shifts from -10dBZ to -5dBZ as cloud parcels go from top to bottom of clouds.

The PDFs of cloud top LWC (Fig. 3.1c), LWP (Fig. 3.1d) and effective radius (Fig. 3.1e) show similar behavior to radar reflectivity in terms of their response to varying cloud geometrical thickness. All three parameters tend to become larger as clouds transition from average to thick clouds. As clouds transition from thick to very thick clouds, the PDFs of these three parameters also change from unimodal to bimodal distributions whose modes are both larger and smaller than that of the average clouds. The behavior of these cloud properties suggests that raindrop embryo production is enhanced through increased cloud droplet sizes and LWC as clouds become thicker from average to thick clouds. It seems that very thick clouds bifurcate into heavy rain with high LWC and light rain with low LWC modes.

In contrast to the other parameters, near cloud top cloud droplet number concentration (Fig. 3.1f) decreases monotonically as clouds become thicker. It seems that the influence of dry air

entrainment and collision-coalescence among cloud droplets tends to become stronger as clouds become thicker.

3.2 Relations between precipitation processes and cloud geometrical thickness

In the previous section, many of the cloud properties were shown to depend on cloud geometrical thickness, which suggests that cloud processes likely depend on cloud geometrical thickness. As summarized in Khain et al. (2008), both model simulations and observational studies show that parcels undergoing different cloud processes can be associated with different sectors of a reflectivity to LWC (Z-R) diagram. In this section, the relationship between precipitation processes and cloud geometrical thickness is explored by examining the distribution of cloud parameters on the Z-LWC diagram. While data are plotted for radar reflectivity from -40 to 10 dBZ, the following discussions focus on the region where radar reflectivity is in the range of -30 to 10 dBZ because the minimum detectable signal of *CloudSat*'s Cloud Profiling Radar (CPR) is approximately -30 dBZ (Marchand et al. 2008).

3.2.1 Probability density distribution

Figure 3.2 shows probability density distributions of satellite-observed subtropical stratocumulus clouds plotted on the Z-LWC diagram for average, thick and very thick clouds, respectively. Dashed, solid and dotted lines are adopted from Khain et al. (2008). Parcels within the clouds move counterclockwise on the Z-LWC diagram. Parcels undergoing condensational growth move rightward along the dashed line. Once cloud droplets become large enough, collision-coalescence among cloud droplets (i.e. autoconversion) is enhanced and parcels move upward along the solid line as rain production begins. The dotted line represents the collection growth of rain embryos while falling through the cloud layer. Parcels move to the lower-left along the dotted line as rain embryos grow by collecting cloud droplets. Observation data are located along the solid line because only data near the cloud top are used in this study.

As expected from Figure 3.1, observational data tends to move to the upper right on the Z-LWC diagram as clouds transition from average to thick clouds. Observational data start to separate into two groups as clouds become very thick. Some clouds move further to the upper right, but the others stay at the lower-middle on the Z-LWC diagram. The result suggests that rain embryo production tends to be enhanced as clouds become thicker, but that these clouds also become more inhomogeneous and divide into drizzling and non-drizzling clouds.

3.2.2 Cloud droplet number concentration

In many bulk microphysics schemes (e.g. Khairoutdinov and Kogan 2000), rain production rate is represented as a function of LWC and cloud droplet number concentration. The relation between cloud droplet number concentration and precipitation processes near cloud top is examined by plotting the mean cloud droplet number concentration on the Z-LWC diagram as shown in Figure 3.3. The mean cloud droplet number concentration shows similar patterns regardless of the cloud geometrical thickness. In general, the mean cloud droplet number concentration is larger for smaller radar reflectivity, which agrees with the bulk representations of autoconversion and accretion processes that rain production rate increases with larger LWC and smaller cloud droplet number concentration.

As expected from Figure 3.1, near cloud top cloud droplet number concentration decreases monotonically as clouds become thicker. It is especially noticeable for clouds with high cloud droplet number concentration (i.e. more than $100cm^{-3}$). It seems that the influence of dry air entrainment and collision-coalescence among cloud droplets tends to become stronger as parcels rise for longer distance within clouds.

3.2.3 Cloud droplets size

Larger cloud droplets enhance raindrop embryo production because collision-coalescence among cloud droplets become more efficient as cloud droplets size increases (e.g. Roger and Yau 1989). In Figure 3.4, the mean cloud droplet effective radius is plotted on the Z-LWC diagram so

as to examine the relation between effective radius and precipitation processes. The mean effective radius shows a similar pattern regardless of cloud geometrical thickness. The mean effective radius tends to be larger for greater LWC and radar reflectivity, which suggests that the rain production rate become more active with larger effective radius.

Figure 3.5 shows the probability density distribution of cloud top radar reflectivity as a function of effective radius for clouds with different geometrical thickness. It seems that cloud top radar reflectivity can be expressed as a single function of cloud thickness and effective radius, which agrees with the previous finding of Rosenfeld et al. (2012) that column maximum rain rate increases with effective radius.

As was also shown in Figure 3.2, the probability density distribution shifts to the upper right on the Z-LWC diagram as clouds transition from average to thick clouds. It starts to separate into drizzling clouds with larger effective radius and non-drizzling clouds with smaller effective radius as the clouds become very thick.

3.2.4 Cloud base radar reflectivity

The above results demonstrate that raindrop embryo generation near cloud top is a function of cloud geometrical thickness, which, in turn, suggests that cloud base rain rate (i.e. rain production within the whole cloud) also depends on cloud geometrical thickness because cloud base rain rate is the result of both raindrop embryo generation and collection growth of raindrop embryos. In Figure 3.6, mean cloud base radar reflectivity is plotted on the Z-LWC diagram so as to investigate the dependence of cloud base rain rate on cloud geometrical thickness and near cloud top raindrop embryos generation.

The mean cloud base radar reflectivity shows a similar pattern for both thick and very thick clouds. A figure for average clouds is not shown because the cloud top and base radar reflectivity are the same by definition in this study. Mean cloud base radar reflectivity is almost entirely determined by cloud top radar reflectivity. It also shows a weak correlation with cloud top LWC as cloud base radar reflectivity increases with higher cloud top LWC.

As shown in Figure 3.7, cloud top LWC can be roughly expressed as a function of LWP. In general, collection growth of raindrop embryos increases as clouds become thicker. While cloud base rain rate is the result of both raindrop embryos generation (i.e. autoconversion) and collection growth of raindrop embryos (i.e. accretion) in warm stratocumulus clouds, Figure 3.6 suggests that cloud base rain rate is mostly determined by the behavior of autoconversion near cloud top.

Cloud base radar reflectivity is slightly higher for thicker clouds at a given cloud top radar reflectivity which demonstrates that accretional growth of rain drops is greater for thicker clouds in general. In order to examine the dependence of accretional growth on cloud geometrical thickness in detail, the mean increase in radar reflectivity from cloud top to base is shown in Figure 3.8. As with Figure 3.6, the mean radar reflectivity increases more for thicker clouds. The spatial patterns of mean radar reflectivity increase (Fig. 3.8) become more similar to those of LWP (Fig. 3.7) in areas with greater LWP (i.e. upper right area in the Z-LWC diagram), which agrees with the notion that the relative contribution of accretional growth to cloud base rain rate should increase with greater LWP. Accretional growth is mostly determined by total cross-sectional area of rain drops, which is correlated to cloud top radar reflectivity in this study, and the total volume of cloud droplets within the column (i.e., LWP). In Figure 3.8, the spatial pattern of radar reflectivity increase changes from a horizontal striped pattern (i.e. radar reflectivity increase is determined by cloud top radar reflectivity) to a pattern that follows the LWP as it moves along the upper-right on the Z-LWC diagram. The transition of the spatial pattern shown in Figure 3.8 indicates that the major factor controlling accretional growth transitions from the total cross-sectional area of rain drops to LWP as the LWP increases.

3.3 Environmental dependence of cloud top properties

As shown in previous sections, near cloud top precipitation processes and cloud base rain rates are largely determined by cloud top properties, especially by cloud droplet size. Rain embryo production rate could be approximately expressed as a function of cloud droplet size. Cloud droplets tend to be larger for clouds with more LWC. As a first-order approximation, near cloud

top LWC is determined by cloud geometrical thickness and adiabatic condensate rate. Atmospheric stability is a key environmental parameter for determining cloud geometrical thickness (Eastman et al. 2017). In this section, the dependence of LWC on adiabatic condensate rate and atmospheric stability is examined.

For this purpose, lower-tropospheric stability (LTS; Klein and Hartman 1993) is used as an indicator for atmospheric stability. LTS is defined as:

$$LTS = \theta_{700} - \theta_{sfc} \tag{3.1}$$

where θ_{700} and θ_{sfc} are the potential temperature at 700hPa and ocean surface, respectively. The adiabatic condensation rate can be approximated as constant within the cloud layer because stratocumulus clouds are relatively thin. The adiabatic condensation rate at cloud base is utilized in this study. Figure 3.9 shows the probability density function (PDF) of adiabatic condensation rate and LTS for average (i.e. geometrical thickness of 144-240m), thick (i.e. geometrical thickness of 384-480m) and very thick (i.e. geometrical thickness of 624-720m) clouds, respectively. Both the adiabatic condensation rate and LTS tend to decrease as clouds become thicker. It is known that LTS has a strong correlation with sea surface temperature in the subtropical stratocumulus regions with LTS decreasing as the sea surface becomes warmer (Klein et al. 1995). Lower LTS deepens the marine boundary layer which leads to thicker stratocumulus clouds. Lower LTS will also lead to higher cloud base heights (lower cloud base temperatures) because the air is warmed by the warmer ocean surface and dried by enhanced entrainment.

Figure 3.10 shows the mean LTS on the Z-LWC diagram. As was show in Figure 3.9, LTS decreases as clouds become thicker. The spatial patterns of LTS are similar for clouds with all geometrical thicknesses. While LTS does not depend on cloud top radar reflectivity, LTS increases with greater cloud top LWC.

The mean adiabatic condensation rate is plotted on the Z-LWC diagram in Figure 3.11. As was shown in Figure 3.9, the adiabatic condensation rate decreases as clouds become thicker. Adiabatic condensation rates show similar spatial patterns for clouds with all geometrical

thicknesses. Similar to LW*C*, the adiabatic condensation rate does not depend on cloud top radar reflectivity but increases with greater cloud top LWC.

Subtropical stratocumulus clouds with higher cloud top LWC tend to have higher adiabatic condensation rates, greater LTS and cloud droplet number concentrations. Higher adiabatic condensation rates are favorable for higher LWC. Greater LTS and cloud droplet number concentrations mitigate the decrease of LWC due to dry air entrainment and precipitation. It seems that subtropical stratocumulus clouds with higher cloud top LWC may exist in an environment that meets the conditions supportive of having high effective condensation rates.

3.4 Summary

In this chapter, the relation between cloud properties (cloud top and base radar reflectivity, cloud top LWC, LWP, near cloud top cloud droplet number concentration and effective radius) and cloud geometrical thickness was investigated by utilizing A-Train satellite observations. The dependence of stratocumulus precipitation processes on cloud geometrical thickness, cloud top properties and environmental parameters was discussed based on their locations on the Z-LWC diagram.

As was found in previous studies, satellite observations show that cloud top LWC and effective radius increase as clouds becomes thicker. However, it was also shown here that clouds become inhomogeneous and separate into two groups as they transition from thick to very thick clouds. Some clouds have higher LWC and larger effective radius, whereas the others have lower cloud top LWC and smaller effective radius. It was also shown that clouds with higher cloud top LWC tend to have higher adiabatic condensation rates, greater LTS and higher cloud droplet number concentrations. It seems that they may exist in an environment that meets the conditions supportive of having high effective condensation rates.

Based upon Z-LWC diagrams, it was suggested that near cloud top raindrop embryo production (i.e. autoconversion) tends to be enhanced as clouds become thicker. It was also suggested that thicker clouds become more inhomogeneous and separate into drizzling and non-

drizzling clouds. From the Z-LWC diagram, mean cloud droplet number concentrations are larger for smaller radar reflectivity, which agrees with typical bulk model representations of autoconversion and accretion processes that the rain production rate increases with larger LWC and lower cloud droplet number concentrations. It was also found that effective radius is a good predictor for cloud top radar reflectivity, which is similar to the findings of Rosenfeld et al. (2012) who noted that column maximum rain rate increases with effective radius. This observational result shows the strong link between autoconversion and effective radius in a more direct manner than the Rosenfeld et al. (2012) study by utilizing cloud top radar reflectivity instead of column maximum reflectivity.

The observation data show that the relative contribution of accretional growth to the cloud base rain rate increases as clouds become thicker. At the same time, it also shows that mean cloud base radar reflectivity is mostly determined by cloud top radar reflectivity, which indicates near cloud top raindrop embryo production. While the cloud base rain rate is the result of autoconversion and accretion in warm stratocumulus clouds, it appears from these results that the cloud base rain rate is mostly determined by the behavior of autoconversion near cloud top.

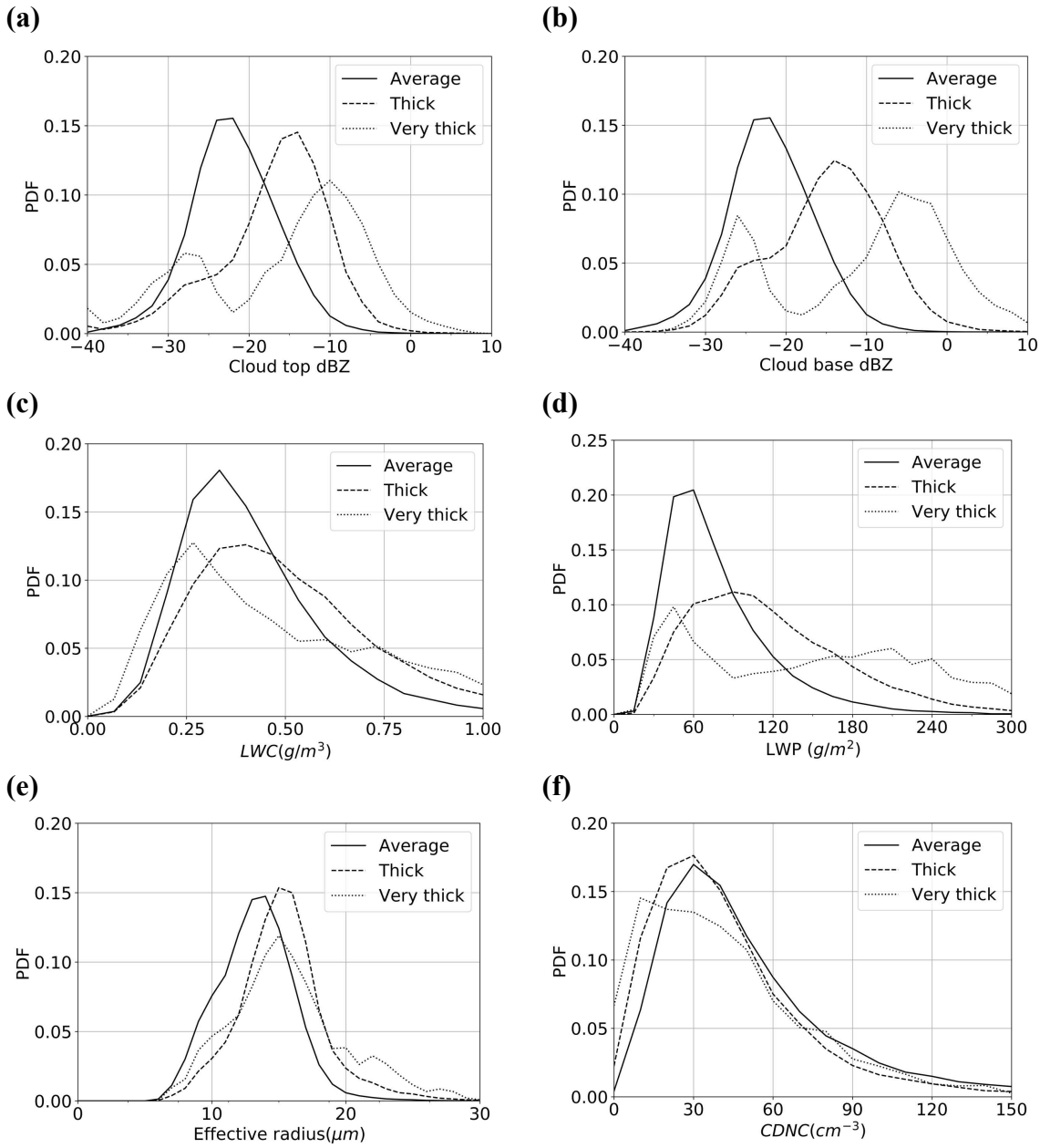

Figure 3.1 Probability density function of (a) cloud top radar reflectivity, (b) cloud base radar reflectivity, (c) cloud top LWC, (d) LWP, (e) cloud effective radius and (f) cloud top cloud droplet number concentration (CDNC) for clouds with geometrical thickness of 144-240m (average), 384-480m (thick) and 624-720m (very thick), respectively.

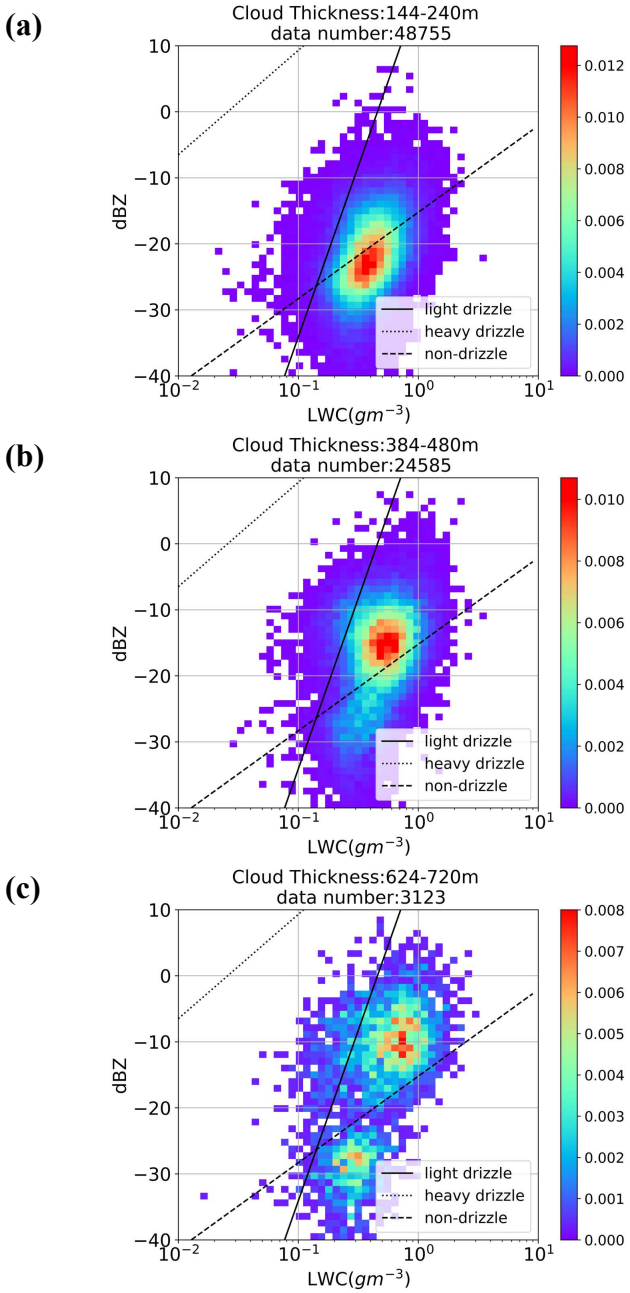

Figure 3.2 Probability density distribution as a function of cloud top radar reflectivity and LWC for clouds with geometrical thicknesses of 144-240m (average), 384-480m (thick) and 624-720m (very thick), respectively.

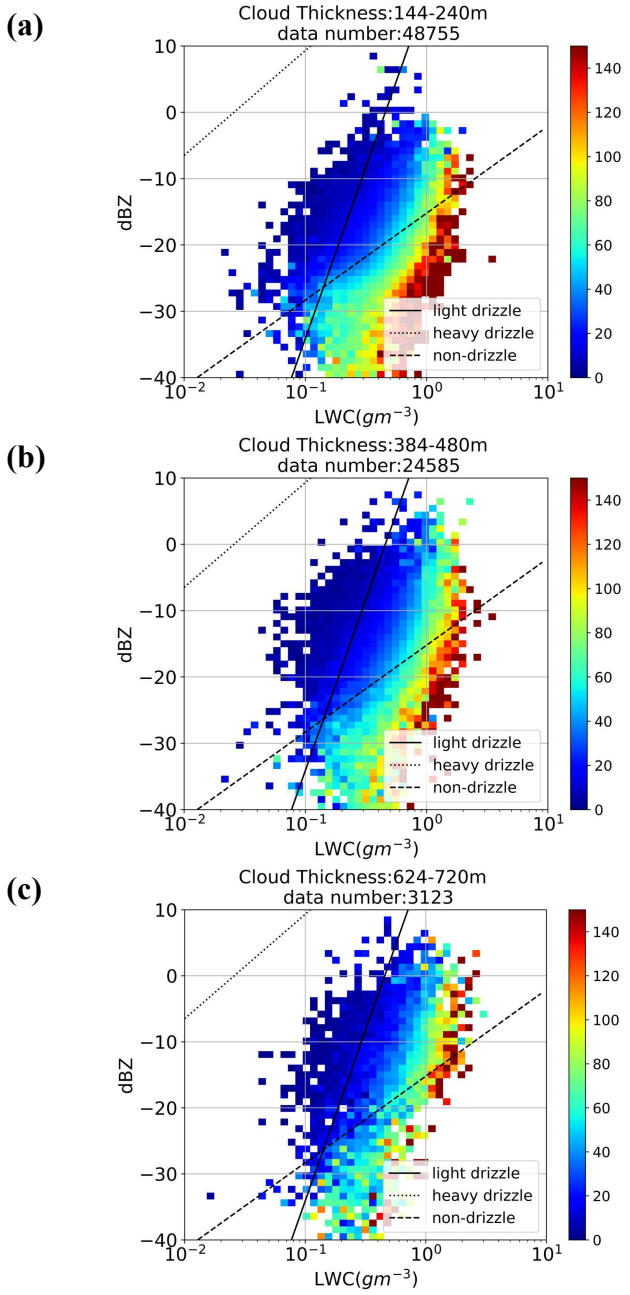

Figure 3.3 Mean cloud top cloud droplet number concentration (cm^{-3}) as a function of cloud top radar reflectivity and LWC for clouds with geometrical thicknesses of (a) 144-240m (average), (b) 384-480m (thick) and (c) 624-720m (very thick), respectively.

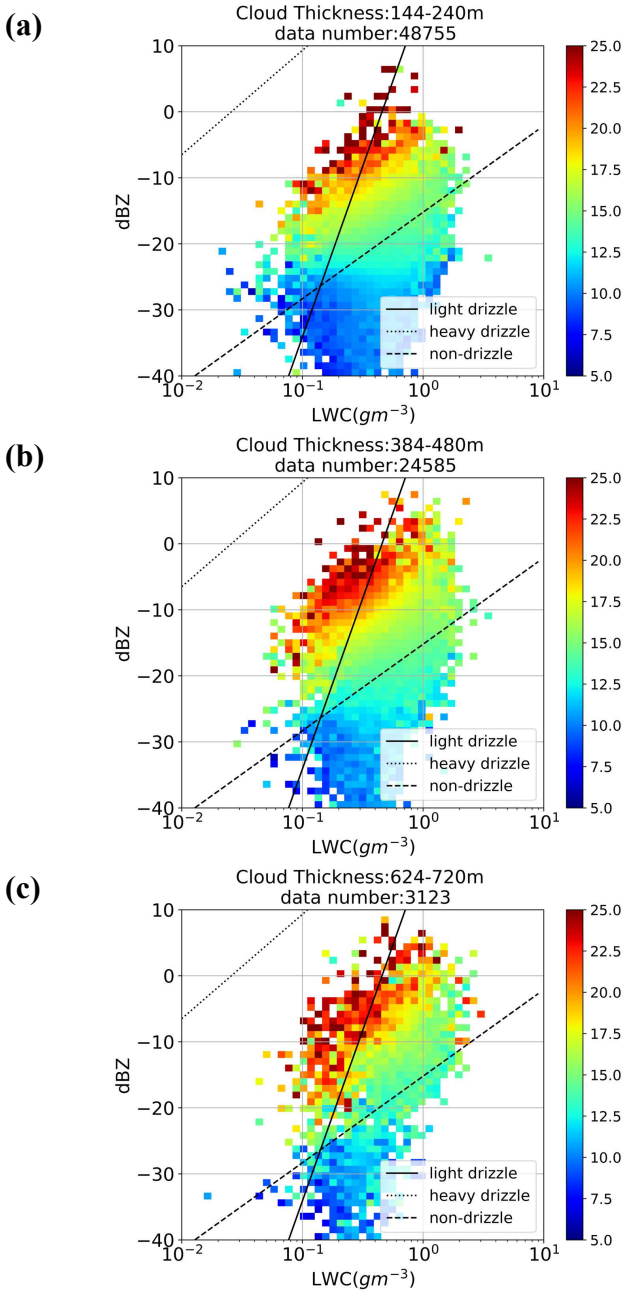

Figure 3.4 Mean cloud top effective radius (μm) as a function of cloud top radar reflectivity and LWC for clouds with geometrical thicknesses of (a) 144-240m (average), (b) 384-480m (thick) and (c) 624-720m (very thick), respectively.

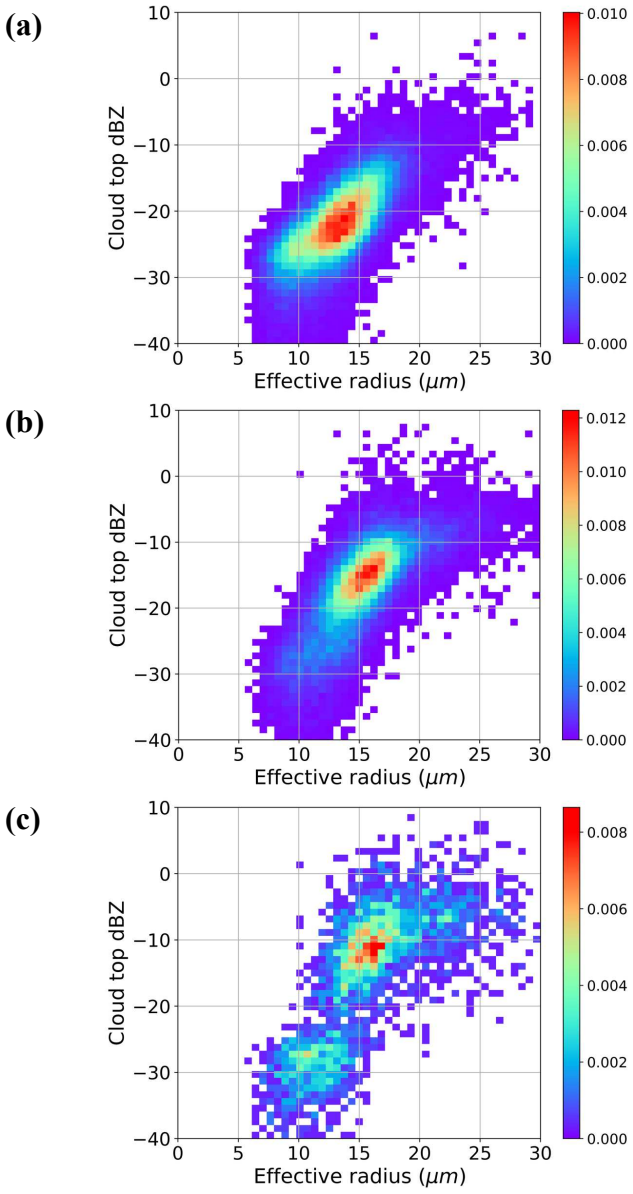

Figure 3.5 Probability density as a function of cloud top radar reflectivity and effective radius for clouds with geometrical thicknesses of (a) 144-240m (average), (b) 384-480m (thick) and (c) 624-720m (very thick), respectively.

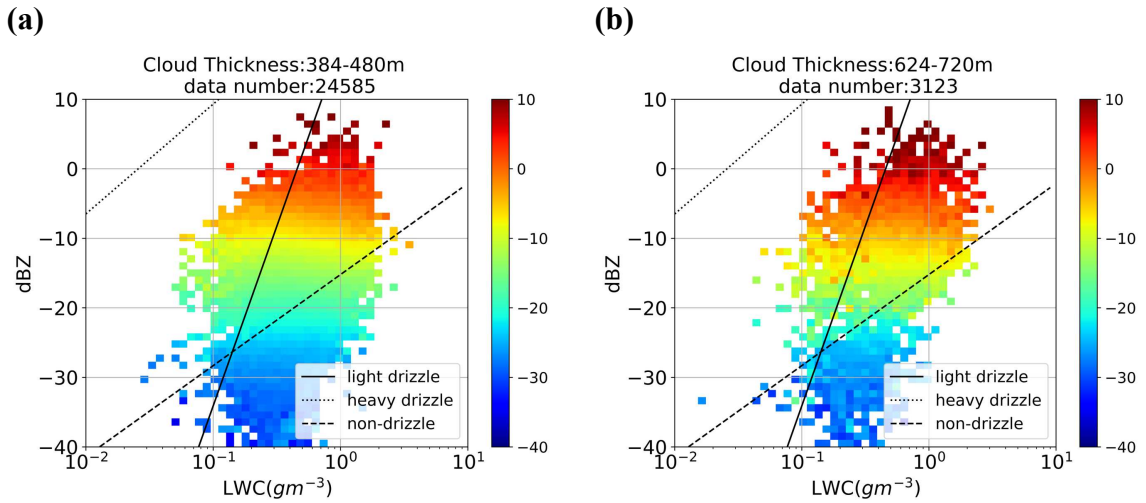

Figure 3.6 Mean cloud base radar reflectivity (dBZ) as a function of cloud top radar reflectivity and LWC for clouds with geometrical thicknesses of (a) 384-480m (thick) and (b) 624-720m (very thick),respectively.

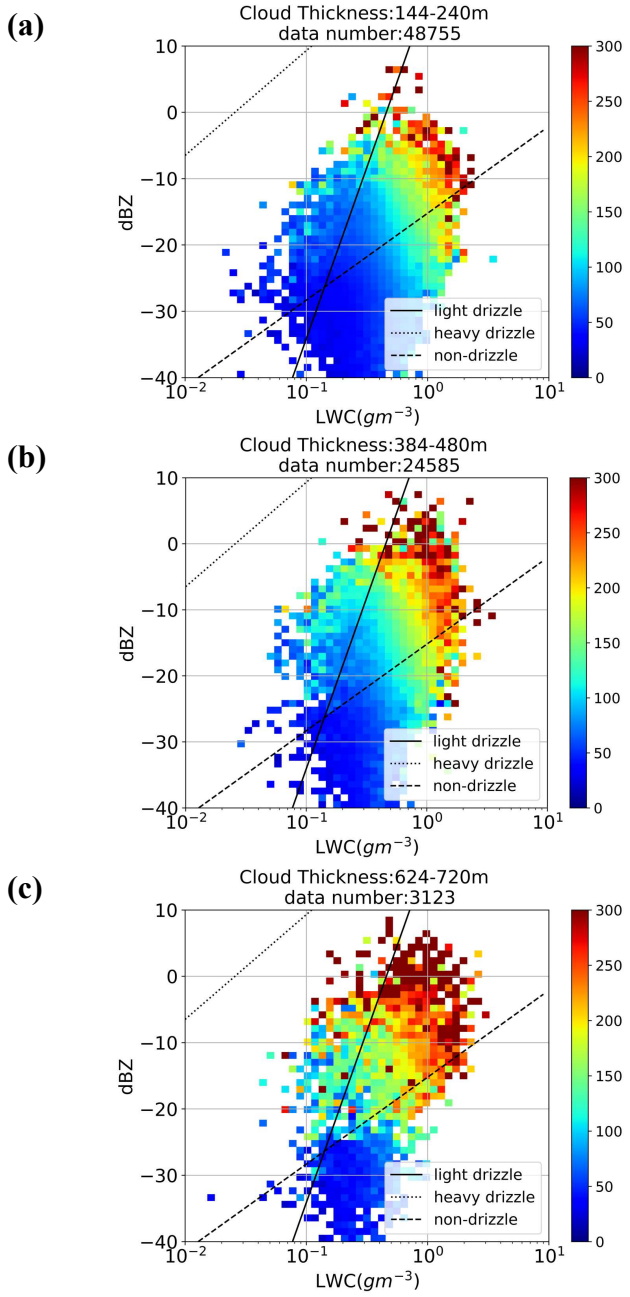

Figure 3.7 Mean LWP (gm^{-2}) as a function of cloud top radar reflectivity and LWC for clouds with geometrical thicknesses of (a) 144-240m (average), (b) 384-480m (thick) and (c) 624-720m (very thick), respectively.

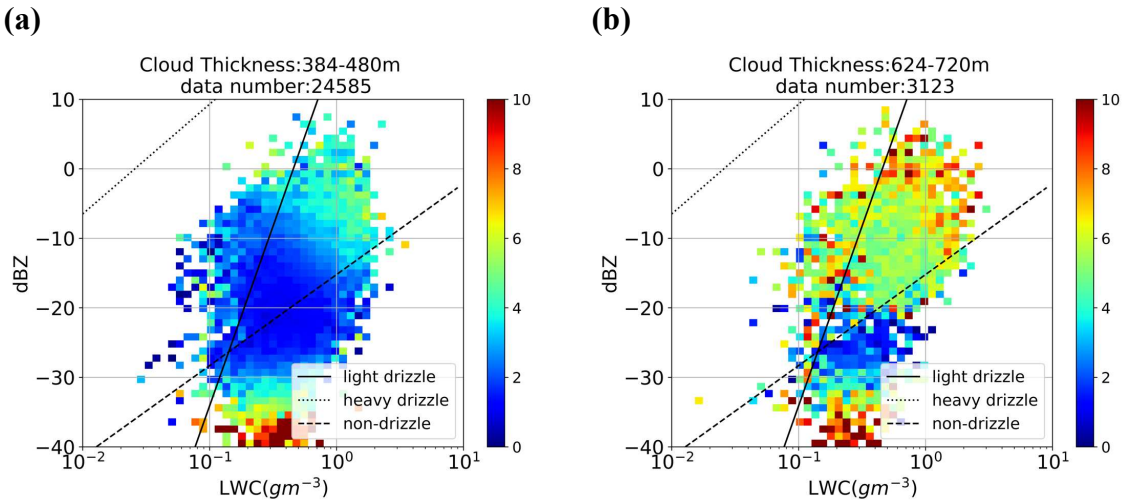

Figure 3.8 Same as Fig. 3.7 but for increase in radar reflectivity (dBZ) from cloud top to base.

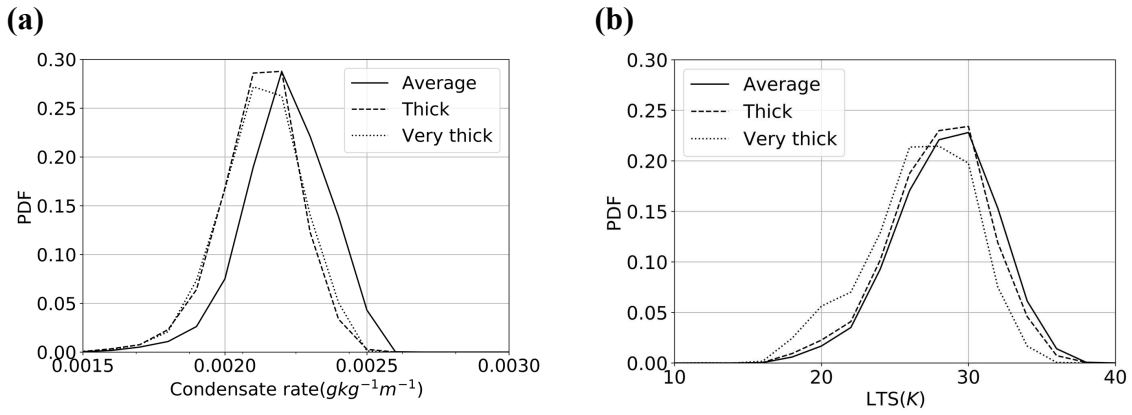

Figure 3.9 Probability density function of (a) adiabatic condensate rate at cloud base and (b) Lower-Tropospheric Stability (LTS) for clouds with geometrical thickness of 144-240m (average), 384-480m (thick) and 624-720m (very thick), respectively.

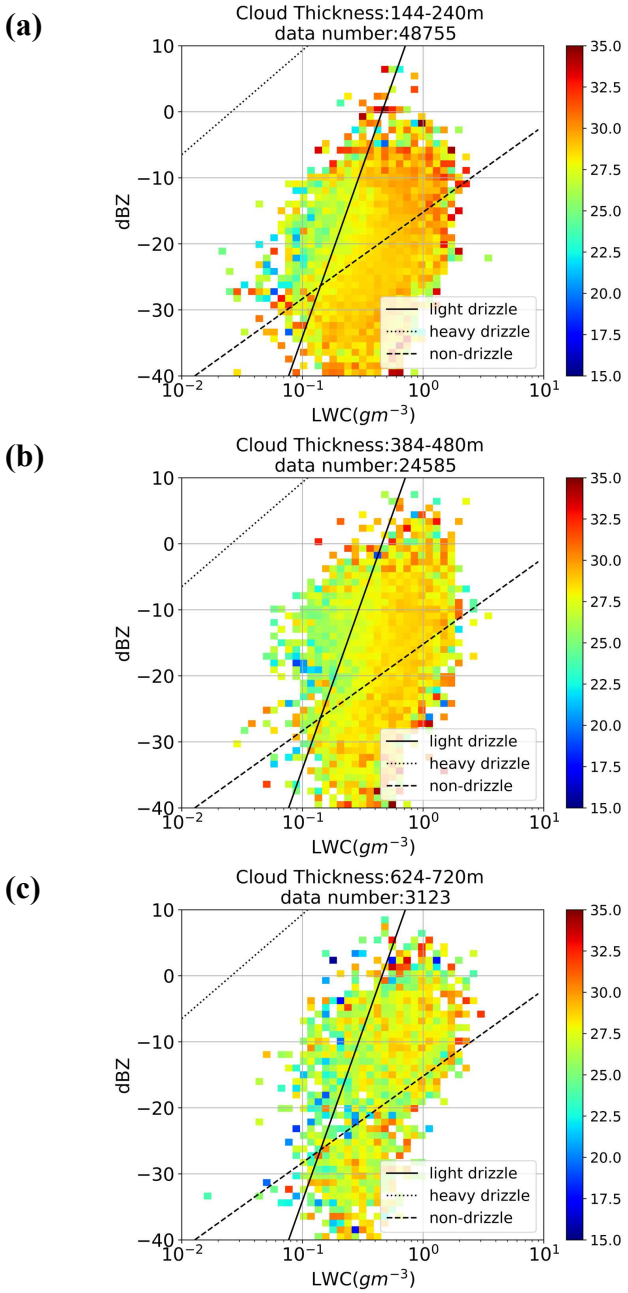

Figure 3.10 Mean LTS as a function of cloud top radar reflectivity and LWC for clouds with geometrical thicknesses of (a) 144-240m (average), (b) 384-480m (thick) and (c) 624-720m (very thick), respectively.

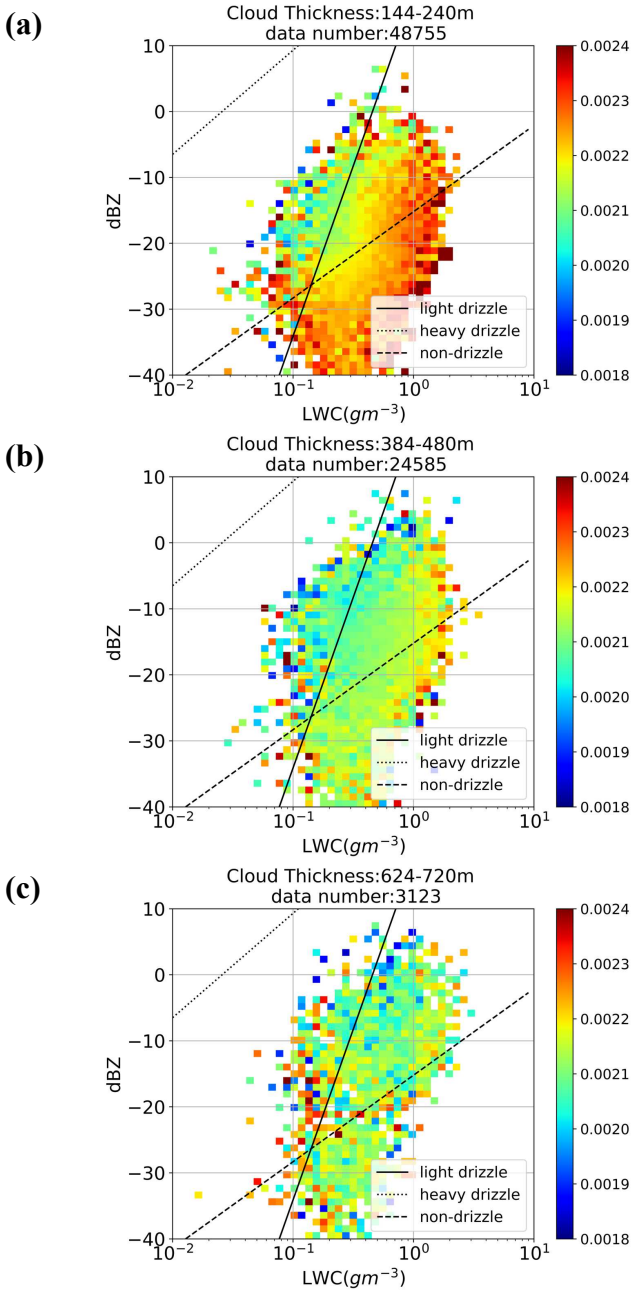

Figure 3.11 Same as Figure 3.10 but for cloud base adiabatic condensation rate.

Chapter 4

Climatology of cloud top properties and their relationships to precipitation generation rate in stratocumulus clouds

4.1 Climatology of cloud properties

Figure 4.1 shows global distributions of mean cloud top LWC, LWP, cloud top and base radar reflectivity and cloud top cloud droplet number concentration for those clouds defined in this study as stratocumulus clouds and passing the quality control procedure described in Chapter 2. The probability density function (PDF) of these parameters for all 8 selected study regions described in Chapter 2 are shown in Figure 4.2. PDFs of cloud top LWC, LWP, cloud top and base radar reflectivity show that stratocumulus clouds fall into two groups: Subtropics (i.e. Northeast Pacific (NEP), Southeast Pacific (SEP), Northeast Atlantic (NEA), Southeast Atlantic (SEA) and Southeast Indian Ocean (SEI)) and Midlatitudes (i.e. North Pacific (NP), North Atlantic (NA) and Sothern Ocean (SO)).

In midlatitude stratocumulus clouds, cloud top radar reflectivity tends to be smaller than that of subtropical stratocumulus. Similarly, cloud base radar reflectivity tends to be smaller for midlatitude stratocumulus clouds compared to their subtropical counterparts. It appears that clouds with heavier (lighter) precipitation at cloud top have heavier (lighter) precipitation at cloud base. In contrast, cloud top LWC and LWP show different trends between the midlatitudes and subtropics. While LWP tends to be greater for midlatitude clouds, cloud top LWC tends to be greater for subtropical clouds. In-situ observations show that LWC increases linearly within the stratocumulus clouds towards the cloud top, which means that clouds with smaller cloud top LWCs need thicker clouds to achieve the given LWP. Effective condensation rates therefore must be smaller for midlatitude clouds because they tend to have smaller cloud top LWC but larger LWP.

PDFs of cloud droplet number concentrations do not show clear differences between subtropical and midlatitude stratocumulus clouds, but the spatial distribution of mean cloud droplet number concentration is different between two groups. Within each subtropical region, the mean cloud droplet number concentration shows a clearly decreasing trend away from shore. This trend

is not found in midlatitude regions where mean cloud droplet number concentrations are relatively similar for both coasts and remote oceans. The spatial pattern of mean cloud droplet number concentration is most pronounced in NEP, SEP and SEA. In these three regions, the spatial distributions of mean cloud top radar reflectivity and cloud droplet number concentrations show opposite patterns. Cloud top radar reflectivity is larger (smaller) for areas with smaller (larger) cloud droplet number concentration.

In contrast, the spatial distribution of cloud top radar reflectivity and LWC shows similar patterns. Both cloud top radar reflectivity and LWC are larger for subtropical clouds than midlatitude clouds. These responses of cloud top radar reflectivity to both cloud top LWC and cloud droplet number concentration are the same as those expected from bulk model microphysical representations of autoconversion, where rain embryo production increases with larger LWC and with smaller cloud droplet number concentrations.

Rain rate is the result of autoconversion and accretion in warm stratocumulus clouds. In general, the contribution of accretional growth to rain rate increases with larger LWP. However, both PDFs and the spatial distributions show that cloud base radar reflectivity is smaller in midlatitudes where the LWP is larger compared to that in the subtropics. Rather, cloud base radar reflectivity shows the same trend as that of cloud top. These results suggest that the cloud base rain rate is determined largely by the behavior of autoconversion near cloud top, which is related to the cloud top radar reflectivity.

4.2 Radar reflectivity as a function of cloud top LWC and cloud droplet number concentration

4.2.1 Cloud top perspective

Figure 4.3 is a scatterplot of cloud top radar reflectivity as a function of cloud top LWC and cloud droplet number concentration. The mean cloud top radar reflectivity for midlatitude and subtropical regions is shown as a function of cloud top LWC and cloud droplet number concentration in Figure 4.4. As expected from Figure 4.1 and 4.2, clouds with higher cloud top radar reflectivity and LWC are found more often in the subtropics compared to the midlatitudes.

Cloud top radar reflectivity shows the same pattern for all 8 regions. Cloud top radar reflectivity is greater for larger LWC and smaller cloud droplet number concentrations. Cloud top radar reflectivity, which has been shown here to be related to rain rate, seems to be represented by the same function of cloud top LWC and cloud droplet number concentration for stratocumulus clouds existing in both subtropics and midlatitude.

4.2.2 Cloud base perspective

Figure 4.5 is a scatterplot of cloud base radar reflectivity shown as a function of cloud top LWC and cloud droplet number concentration. The mean cloud base radar reflectivity for midlatitude and subtropical regions is shown as a function of cloud top LWC and cloud droplet number concentration in Figure 4.6. Comparison between Figures 4.4 and 4.6 indicates that the cloud base radar reflectivity is greater than that at cloud top for a given cloud top LWC and cloud droplet number concentration. This tendency becomes more prominent for clouds with greater radar reflectivity while it is not clear for clouds with radar reflectivity below approximately -20 dBZ.

As was observed for the case for cloud tops, the cloud base radar reflectivity patterns are the same for all 8 regions. Clouds with higher cloud base radar reflectivity and LWCs are found more frequently in the subtropics compared to midlatitudes. It seems that cloud base radar reflectivity can also be expressed as a single function of cloud top LWC and cloud droplet number concentration for stratocumulus clouds existing in both the subtropics and midlatitudes, although the relationship does differ from that for cloud top radar reflectivity.

4.2.3 Radar reflectivity as a function of LWP and cloud top cloud droplet number concentration

Leon et al. (2008) examined how cloud base radar reflectivity can be parameterized as a function of LWP and cloud top cloud droplet number concentration by combining *CloudSat* and MODIS observations. They found that cloud base radar reflectivity should be parameterized differently for midlatitude and subtropical stratocumulus clouds, which seems inconsistent with

the result shown in the previous subsection. In this subsection, cloud radar reflectivity is examined as a function of LWP and cloud top cloud droplet number concentration, with a focus on the differences between midlatitude and subtropical regions.

Figure 4.7 is a scatterplot of cloud top radar reflectivity shown as a function of LWP and cloud droplet number concentration for each of the stratocumulus regions. Mean values for midlatitude and subtropical regions are shown in Figure 4.8. Note that the color scale of radar reflectivity is the same as that for Figures 4.3 to 4.6. Although cloud top radar reflectivity increases with grater LWP and smaller cloud droplet number concentration in all 8 regions, its value and pattern show noticeable differences between the subtropics and midlatitudes.

As expected from Figure 4.1 and 4.2, cloud top radar reflectivity is larger for subtropical clouds with given LWP and cloud droplet number concentrations in general. While midlatitude clouds with cloud top radar reflectivity exceeding -10dBZ can be found in limited areas of the LWP-cloud droplet number concentration (LWC-CDNC) plane, cloud top radar reflectivity of subtropical clouds exceeds -10dBZ can be found in wide areas of the LWC-CDNC plane. From this perspective, radar reflectivity must be parameterized differently for midlatitude and subtropical stratocumulus clouds when LWP and cloud droplet number concentration are used as explanatory variables, which is in agreement with the findings of Leon et al. (2008).

4.2.4 Controlling factors for accretional growth

Figures 4.9 and 4.10 are the same as Figures 4.7 and 4.8, but are for cloud base radar reflectivity. Radar reflectivity is generally greater at cloud base, but its spatial pattern in the LWP-CDNC plane is similar at both cloud top and base for each of the 8 regions. To illuminate how accretional growth varies with LWP and cloud top cloud droplet number concentration, the radar reflectivity increase from cloud top to base is plotted on the LWP-CDNC plane in Figure 4.11, and Figure 4.12 shows mean values for the midlatitude and subtropical regions.

Accretional growth is primarily determined by the product of collision-coalescence efficiency between collector (i.e., rain) drops and collected (i.e., cloud) droplets, total cross-

sectional area of rain drops and total volume of cloud droplets within the column (i.e., LWP). Since the spatial pattern of accretional growth on the CDNC-LWP plane is similar to those of the radar reflectivity rather than being parallel to CDNC-axis, these results suggest that accretional growth of rain drops in stratocumulus clouds depends more on total cross-section of rain drops and less on LWP.

4.3 Discussion

Unlike observational studies that have focused primarily on LWP and cloud droplet number concentration (e.g. Comstcok et al. 2004), cloud parameterization studies have typically focused on cloud top LWC and cloud droplet number concentrations (e.g. Liu and Daum 2004). Many bulk model microphysics parameterizations have been proposed based on different assumptions regarding the cloud droplet size distributions (e.g. Berry and Reinhardt 1974; Khairoutdinov and Kogan 2000), but the results presented in the previous section indicate that the autoconversion process can indeed be represented with a globally applicable function of cloud top LWC and cloud droplet number concentration for all warm stratocumulus clouds. In this section, the dependence of cloud top rain rate on cloud top LWC and cloud droplet number concentration are explored quantitatively. These results will constitute a behavior that numerical weather models should reproduce because precipitation processes (i.e. autoconversion and accretion) are expressed as function of LWC and cloud droplet number concentration in many bulk microphysics schemes used in these models.

A reflectivity to rain rate (Z-R) relation shown in Eq. (4.1) is employed to estimate cloud top rain rate from cloud top radar reflectivity observed by *CloudSat*:

$$Z = 25R^{1.3} \tag{4.1}$$

where Z and R have units of $mm^6\, m^{-3}$ and $mm\, d^{-1}$, respectively. Comstock et al. (2004) obtained this relation based on ground-based radar and aircraft observations of southeast Pacific stratocumulus clouds from the East Pacific Investigation of Climate (EPIC) field campaign. It is applied here for subtropical stratocumulus clouds with radar reflectivity between $-25\, dBZ$ to

10 dBZ, corresponding to the range for which they were originally derived. Thus, the analysis is limited to subtropical stratocumulus clouds in this section.

4.3.1 Sensitivity of precipitation generation rate to LWC

Figure 4.13 shows the probability density of cloud top rain rate as a function of LWC. Cloud top rain rate, which is an indicator of precipitation generation rate near cloud top, becomes more enhanced with increasing cloud top LWC.

In order to examine how the relation between cloud top rain rate and LWC changes with varying cloud droplet number concentration, the probability density of cloud top rain rate as a function of LWC is further separated for clouds with cloud top cloud droplet number concentration of $15-25\ cm^{-3}$ and $35-45cm^{-3}$. This is shown in Figure 4.14. For each subset, principal component analyses (PCAs) were conducted to find the vector which best explains the relation between cloud top rain rate(R_{ct}) and cloud top LWC using a logarithmic coordinate. The black dashed lines indicate the first principal component of the PCA, which has a slope of $R_{ct} \propto LWC^{3.92}$ and $R_{ct} \propto LWC^{3.42}$ for cloud droplet number concentration of $15-25\ cm^{-3}$ and $35-45cm^{-3}$, respectively. Clouds with fewer cloud droplet number concentration (i.e., larger cloud droplets sizes) tend to have larger cloud top rain rates. Lower cloud droplet number concentrations enhance the autoconversion rate and produce more rain drops for a given LWC. More rain drops also enhance the rain drop growth. As a result, lower cloud droplet number concentrations lead to greater rain drop production.

Cloud top rain rates of clouds with lower cloud droplet number concentrations are also more sensitive to changes in cloud top LWC. The collision-coalescence efficiency between liquid water droplets, as well as the fall speed of those droplets, increases with droplet size. Thus, enhancement of autoconversion and accretion is more evident in clouds with larger cloud droplet sizes.

4.3.2 Sensitivity of precipitation generation rate to cloud droplet number concentration

Figure 4.15 shows the distribution of cloud top rain rate as a function of cloud droplet number concentration. Cloud top rain rate increases with decreasing cloud droplet number concentration, most likely because larger cloud droplets enhance the raindrop embryo production near cloud top.

Figure 4.16 shows the distribution of cloud top rain rate (R_{ct}) as a function of cloud top cloud droplet number concentration (N_d) for clouds with cloud top LWC of $0.25-0.35\ gm^{-3}$ and $0.40-0.50 gm^{-3}$, respectively. The black dashed lines indicate the first principal component of the PCA, which has a slope of $R_{ct} \propto {N_d}^{-1.51}$ and $R_{ct} \propto {N_d}^{-1.89}$ for cloud top LWC of $0.25-0.35\ gm^{-3}$ and $0.40-0.50 gm^{-3}$, respectively.

The responses of cloud top rain rate to varying cloud top LWC and cloud droplet number concentrations obtained from satellite observation become more (less) sensitive for cloud with stronger (weaker) cloud top rain rare.

4.3.3 Validity of quasi-stationary clouds assumption

In the above discussions, it is assumed that each subtropical stratocumulus cell is in quasi-steady state. If clouds are not in quasi-steady state, the cloud top rain rate might not be representative of near cloud top rain production (i.e. sum of autoconversion and accretion rate). In order to examine the validity of the steady state assumption, the time evolution of LWP for stratocumulus clouds at SEP region is shown in Figure 4.17. Little temporal change is evident over the hour shown. Given the persistence of stratocumulus clouds in these regions, and little apparent change over one hour, we assume that quasi-steady assumption can be applied.

4.4 Summary

In this chapter, the climatology of satellite-derived cloud properties for 8 stratocumulus cloud regions are presented with the focus on exploring similarities and differences among stratocumulus clouds developing in subtropical and midlatitude regions. Responses of cloud top and base radar reflectivity to cloud top LWC, cloud droplet number concentration and LWP are

also investigated and their implications for the parameterization of stratocumulus precipitation processes within bulk microphysical models is discussed.

As was found in previous studies, the climatology of cloud properties was found to be different between subtropical and midlatitude stratocumulus clouds. While LWP tends to be larger for midlatitude clouds, cloud top LWC and both cloud top and base radar reflectivity tends to be larger for subtropical stratocumulus clouds. A PDF of cloud droplet number concentration does not show clear differences between subtropical and midlatitude stratocumulus cloud droplet number concentration, but individual regions do show clear spatial differences. While mean cloud droplet number concentration shows a clearly decreasing trend away from shore within each subtropical region, there is no significant contrast between the coast and remote ocean within each midlatitude region. This spatially inhomogeneous pattern of mean cloud droplet number concentration is most pronounced in NEP, SEP and SEA. In these three regions, cloud top radar reflectivity is larger (smaller) for areas with smaller (larger) cloud droplet number concentration. These responses of cloud top radar reflectivity to both cloud top LWC and cloud droplet number concentration are consistent with those expected from bulk microphysics representations of autoconversion where raindrop embryo production increases with larger LWC and smaller cloud droplet number concentrations.

It was shown that cloud top and base radar reflectivity could be parameterized as a function of cloud properties. Cloud base radar reflectivity was found to depend on LWP and cloud droplet number concentration but the expression needs to be differentiated between midlatitude and subtropical regions. This agrees with the findings of previous observational study (Leon et al. 2008). It was also shown that cloud top radar reflectivity can be parameterized as a function of LWP and cloud droplet number concentration with a similar manner as those for cloud base radar reflectivity.

In contrast, it was shown that cloud top radar reflectivity can be parameterized with a globally uniform relation when represented as a function of cloud top LWC and cloud droplet number concentration. This is consistent with the bulk representation of autoconversion and

accretion processes in typical bulk microphysical models. While falling through the cloud, rain drops become larger by accretional growth which is proportional to LWP. However, the results suggest that cloud base radar reflectivity can be also represented by a globally applicable parameterization as a function of cloud top LWC and cloud droplet number concentration. Comparing the response of cloud top radar reflectivity (Z_{ct}) and the increase in radar reflectivity from cloud top to bottom ($Z_{cb} - Z_{ct}$) with respect to LWP and cloud droplet number concentration, it was found that the accretional growth is correlated to cloud top radar reflectivity. Although accretional growth is controlled by both total cross-sectional area of rain drops and LWP in general, these results show that it depends more on the total cross-sectional area of rain drops and less on LWP in stratocumulus clouds.

Finally, the responses of cloud top rain rate to varying cloud top LWC and cloud droplet number concentration were investigated. It was shown that cloud top rain rate is more (less) sensitive to changes in LWC and cloud droplet number concentration for cloud with stronger (weaker) cloud top rain rate. This agrees with the fact that collision-coalescence efficiency between liquid water droplets with the size of cloud droplets (i.e. approximately 20 μm in diameter) increases non-linearly with droplet size (e.g. Hall 1980).

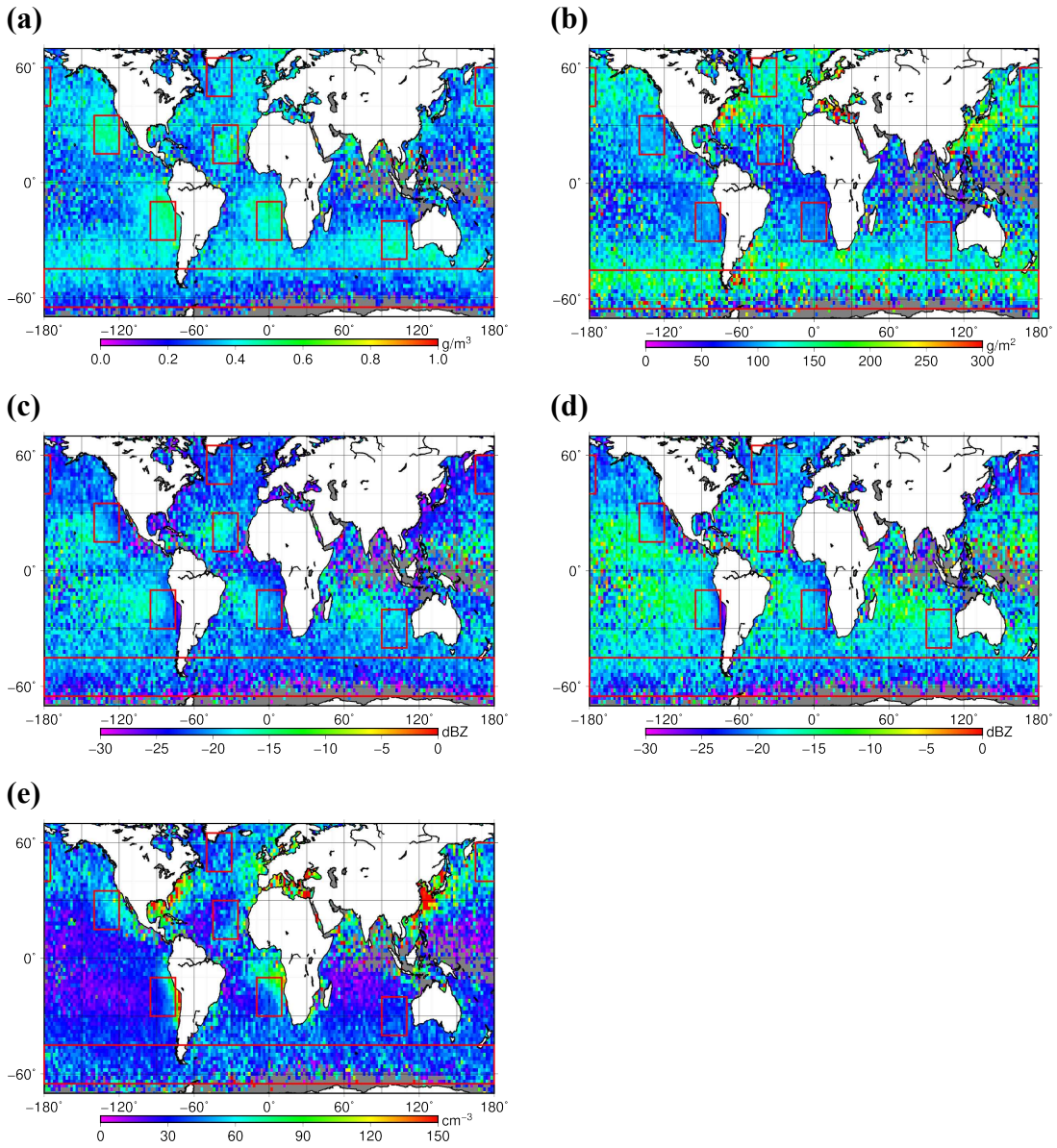

Figure 4.1 Global distribution of mean cloud properties for warm maritime stratocumulus clouds. (a)cloud top LWC(gm^{-3}), (b)LWP(gm^{-2}), (c) cloud top radar reflectivity(dBZ), (d) cloud base radar reflectivity(dBZ), (e)cloud droplet number concentration(cm^{-3}). Regions enclosed in red rectangles indicate the analysis regions.

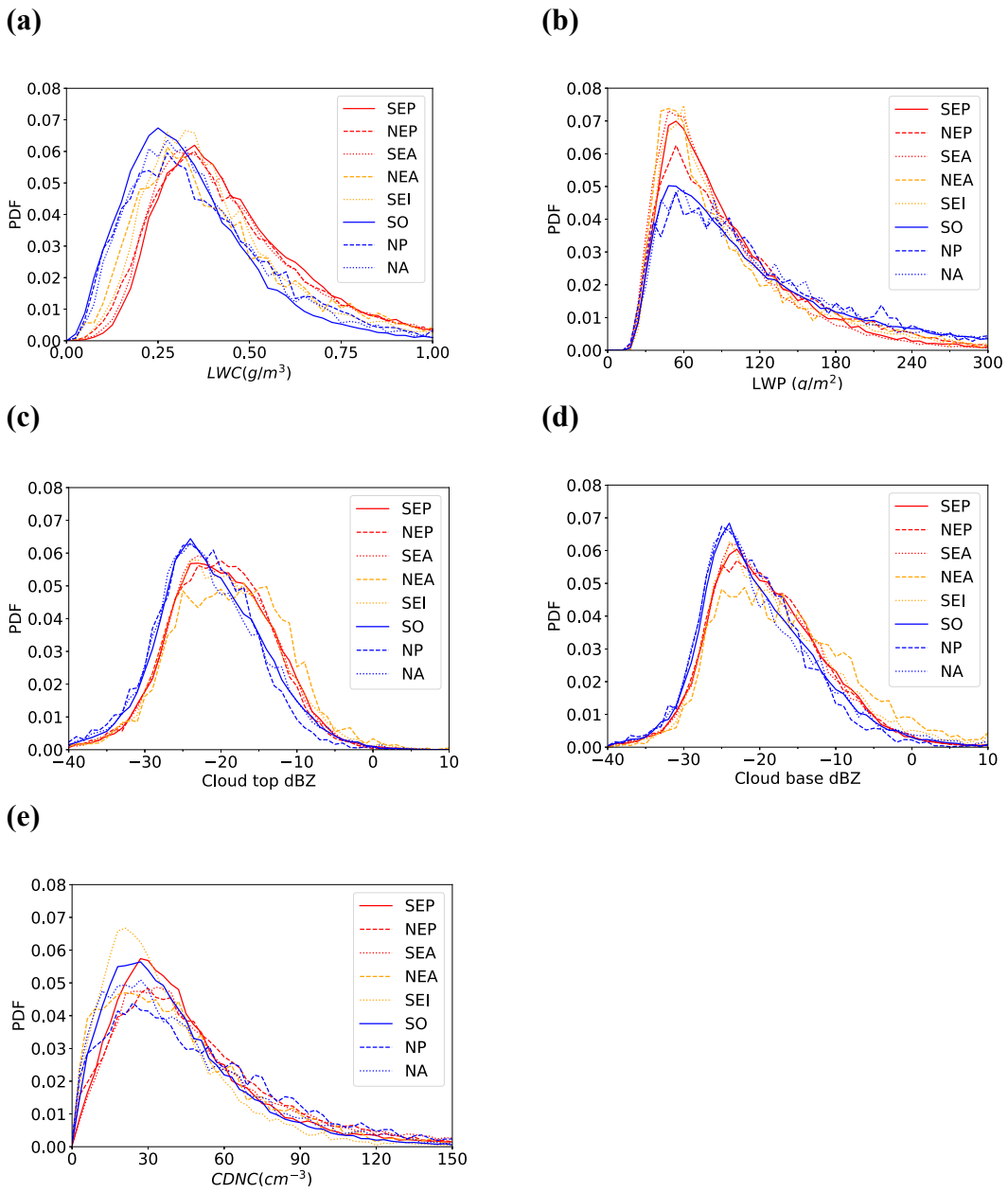

Figure 4.2 Probability density function of (a) cloud top LWC(gm^{-2}); (b) LWP(gm^{-3}); (c) cloud base radar reflectivity (dBZ); (d) cloud top radar reflectivity (dBZ); and (e) cloud droplet number concentration(cm^{-3}) for eight analysis regions.

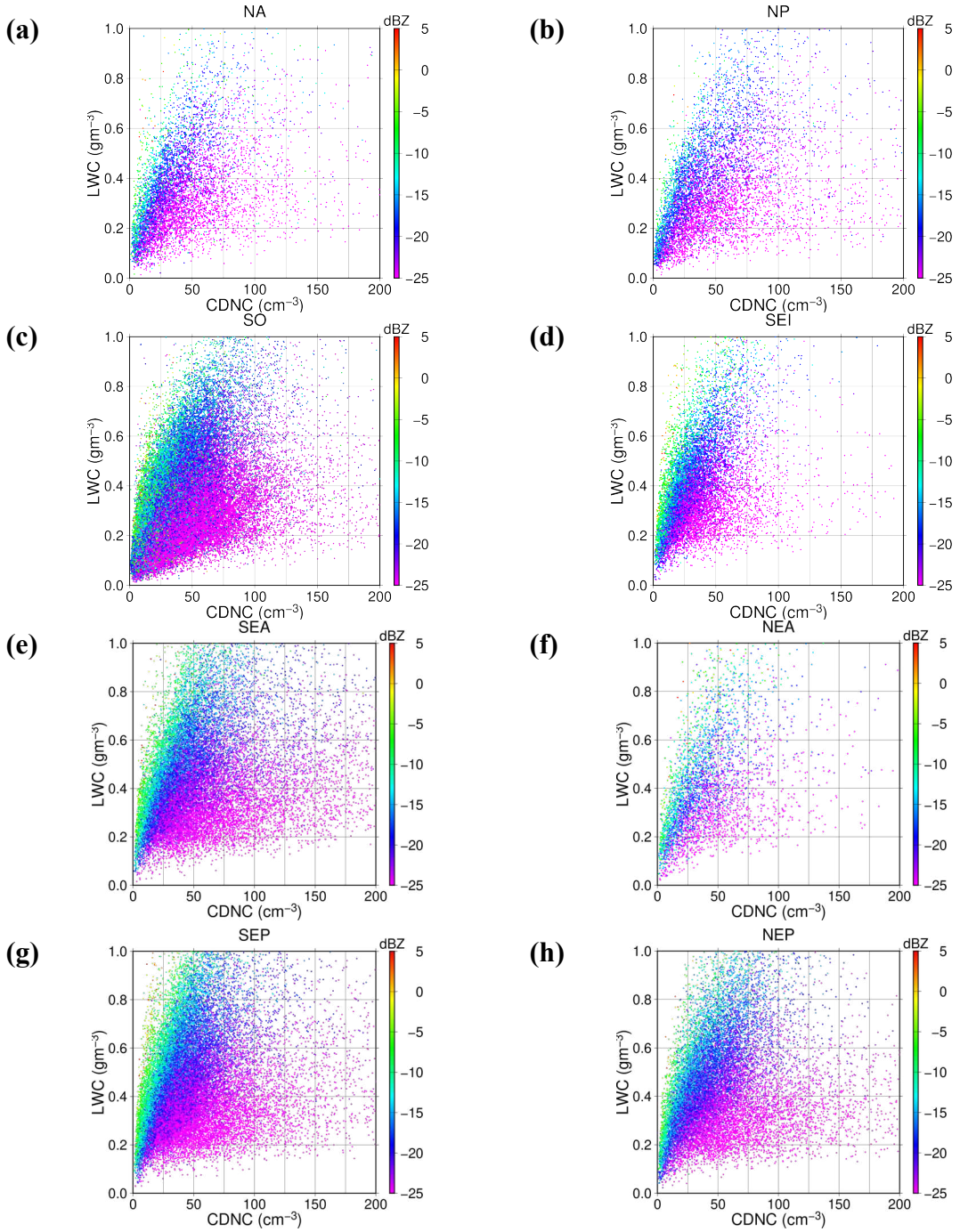

Figure 4.3 Scatterplot of cloud top radar reflectivity(dBZ) as a function of cloud droplet number concentration(CDNC)(cm^{-3}) and cloud top LWC(gm^{-3}) for (a) NA, (b) NP, (c) SO, (d) SEI, (e) SEA, (f) NEA, (g) SEP, (h) NEP.

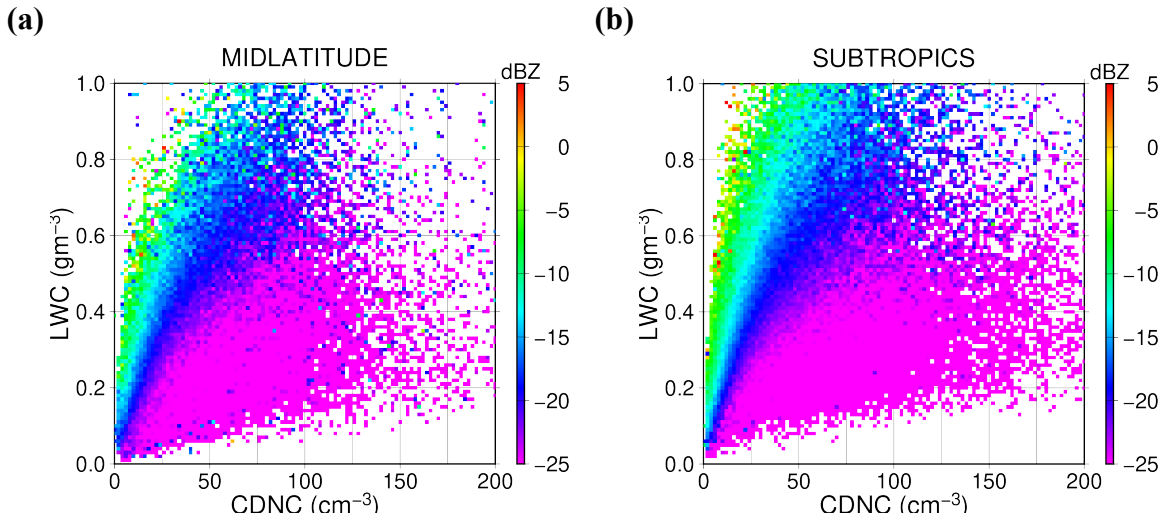

Figure 4.4 Mean cloud top radar reflectivity as a function of cloud top LWC(gm^{-3}) and cloud droplet number concentration(CDNC)(cm^{-3}) for (a) midlatitude and (b) subtropical regions.

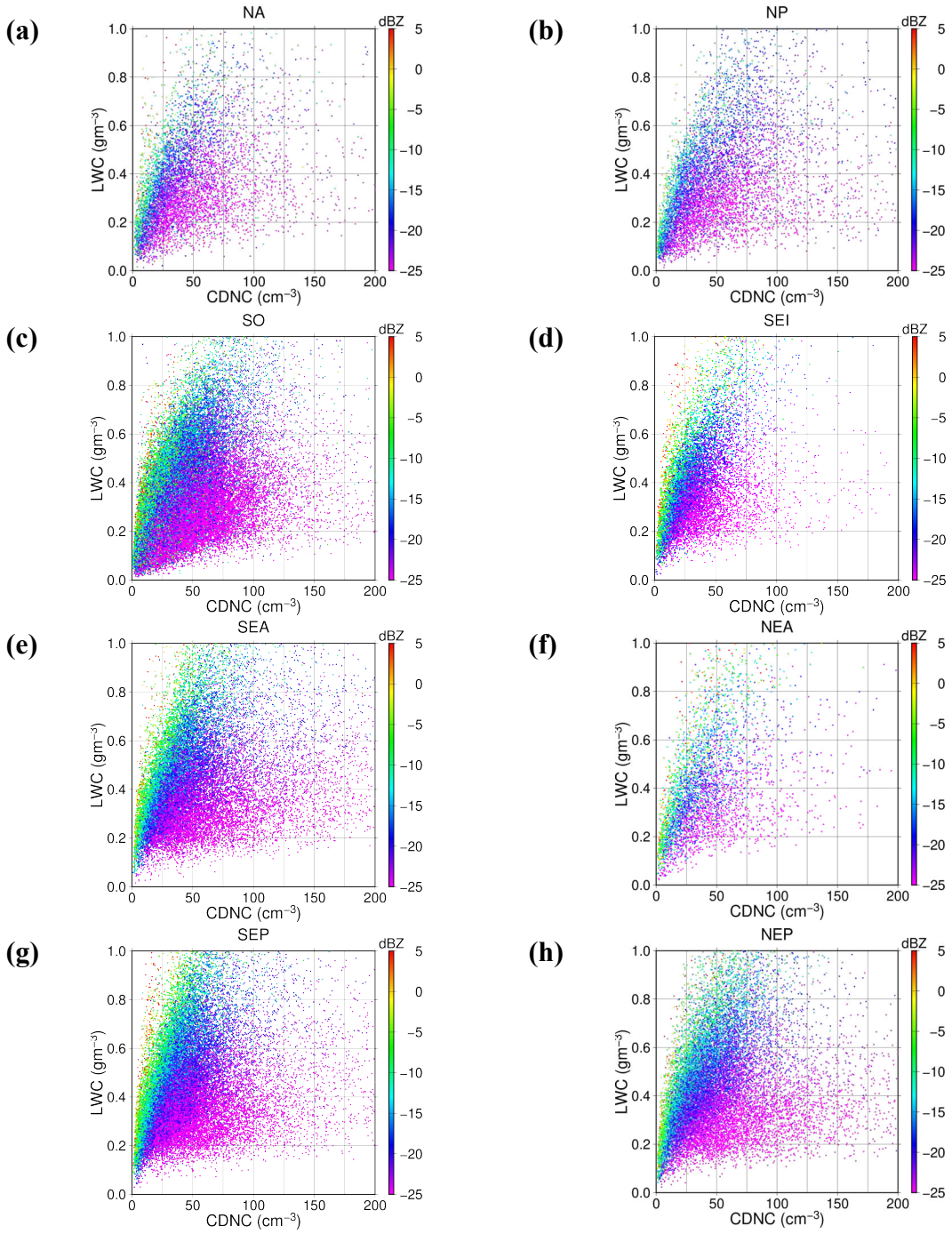

Figure 4.5 Same as Figure 4.3 but for cloud base radar reflectivity.

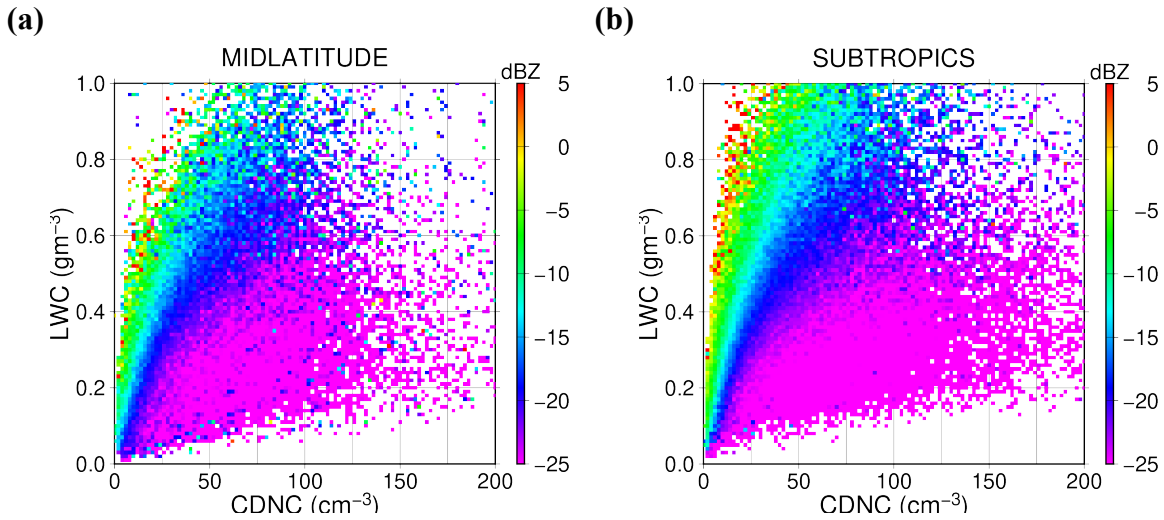

Figure 4.6 Same as Figure 4.4 but for cloud base radar reflectivity.

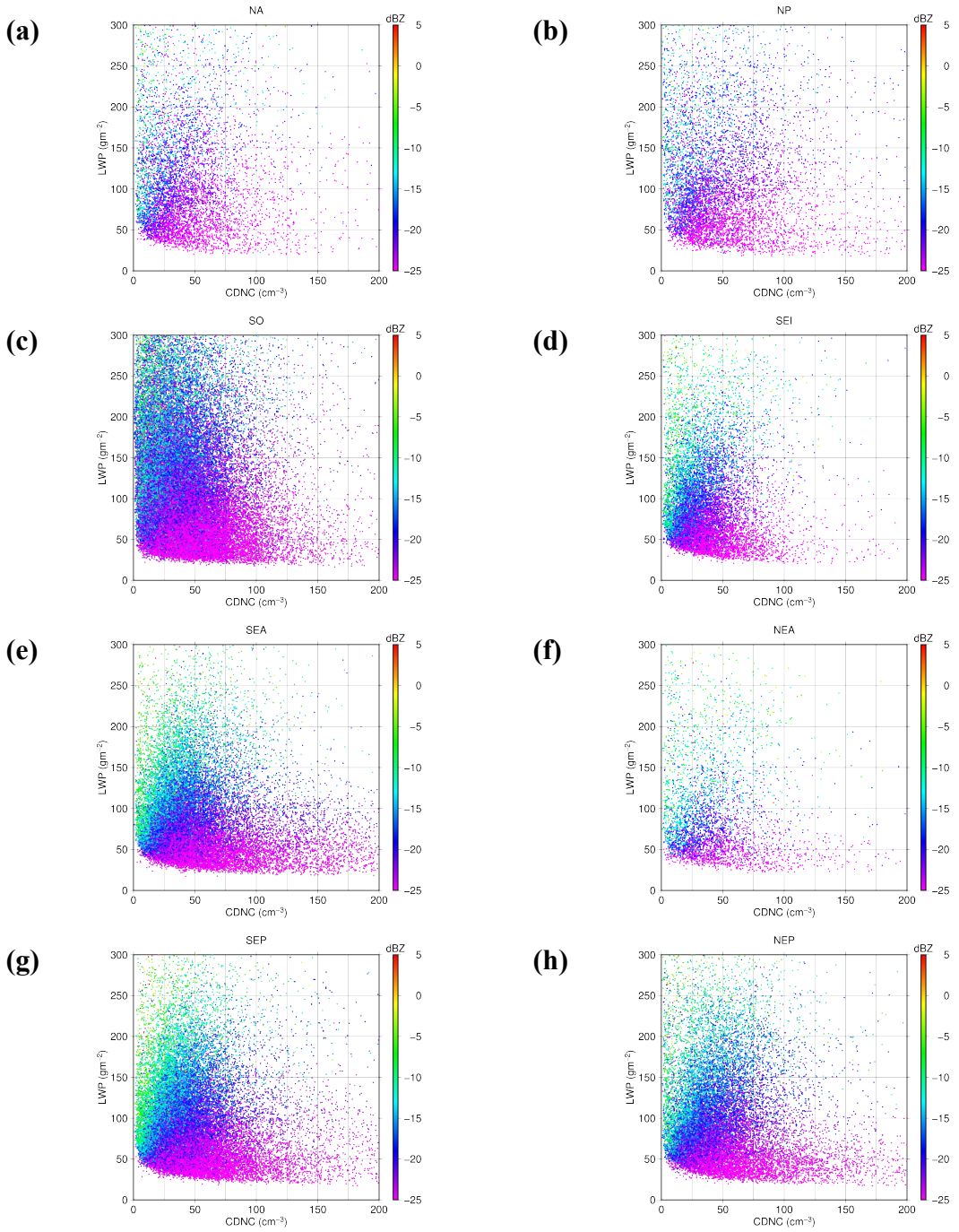

Figure 4.7 Scatterplot of cloud top radar reflectivity(dBZ) shown as a function of LWP(gm^{-2}) and cloud droplet number concentration(CDNC) (cm^{-3}) for (a) NA, (b) NP, (c) SO, (d) SEI, (e) SEA, (f) NEA, (g) SEP, (h) NEP.

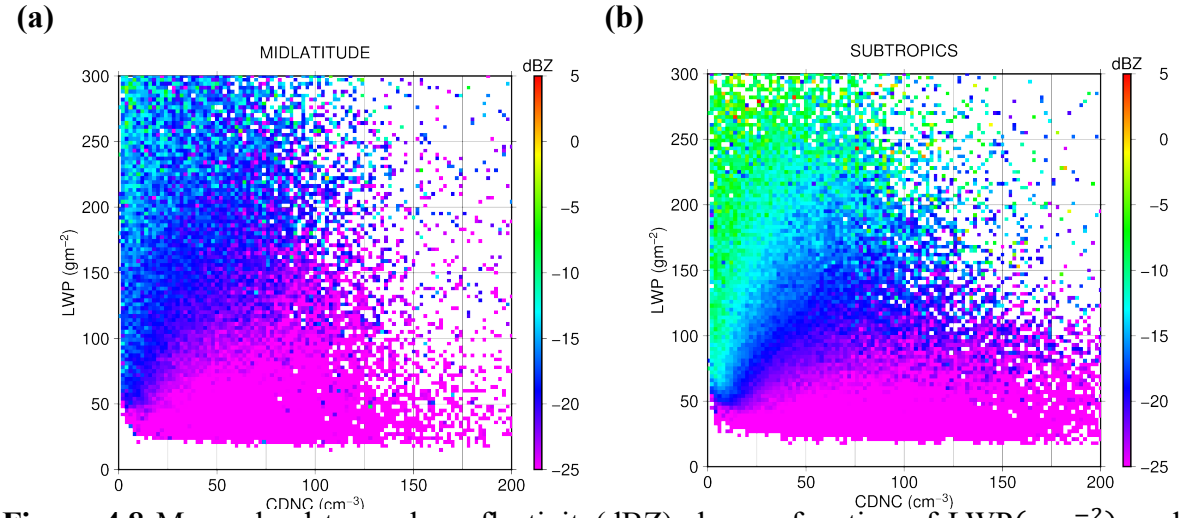

Figure 4.8 Mean cloud top radar reflectivity(dBZ) ~~sh~~ as a function of LWP(gm^{-2}) and cloud droplet number concentration(CDNC)(cm^{-3}) for (a) midlatitude and (b) subtropical regions.

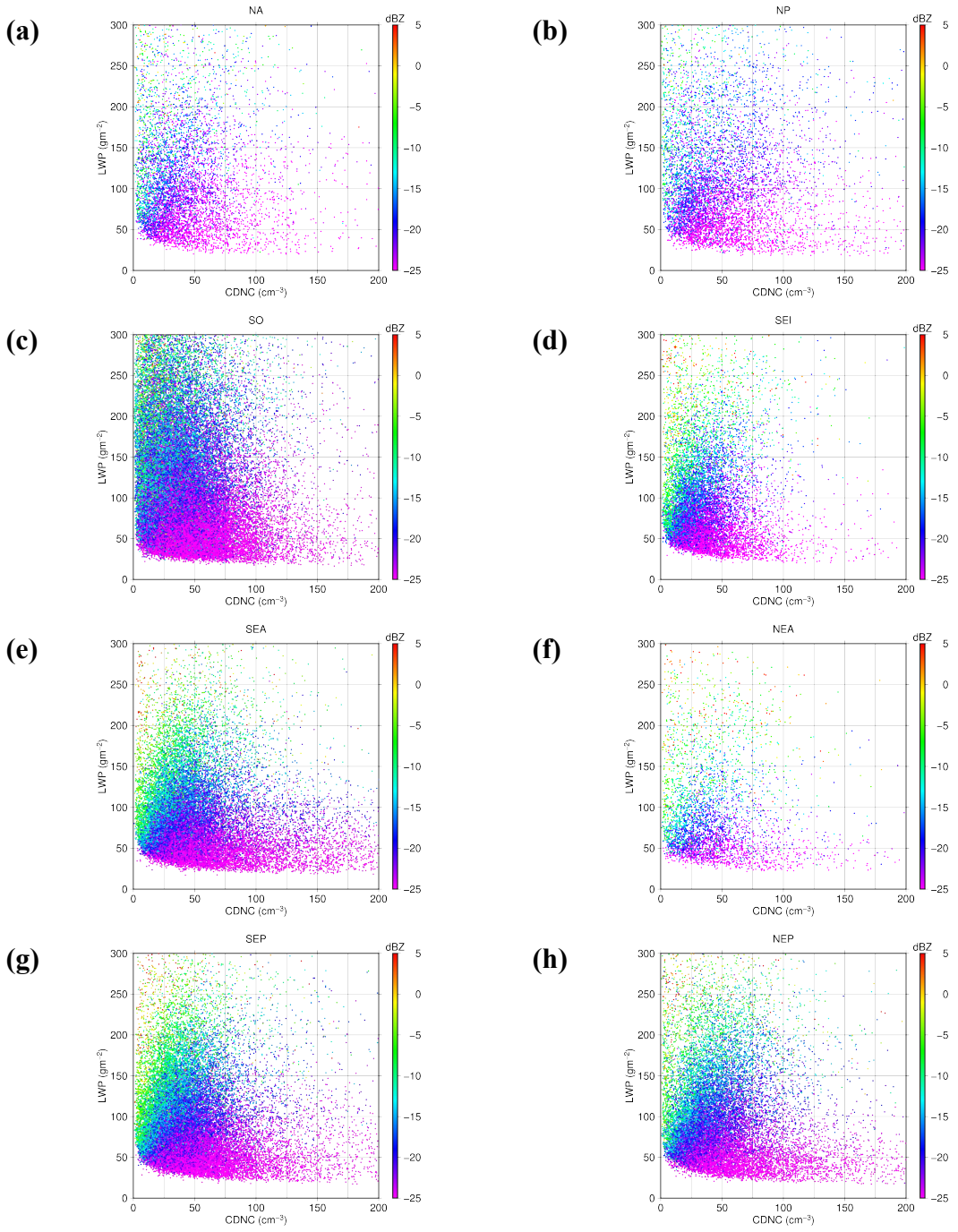

Figure 4.9 Same as Figure 4.7 but for cloud base radar reflectivity.

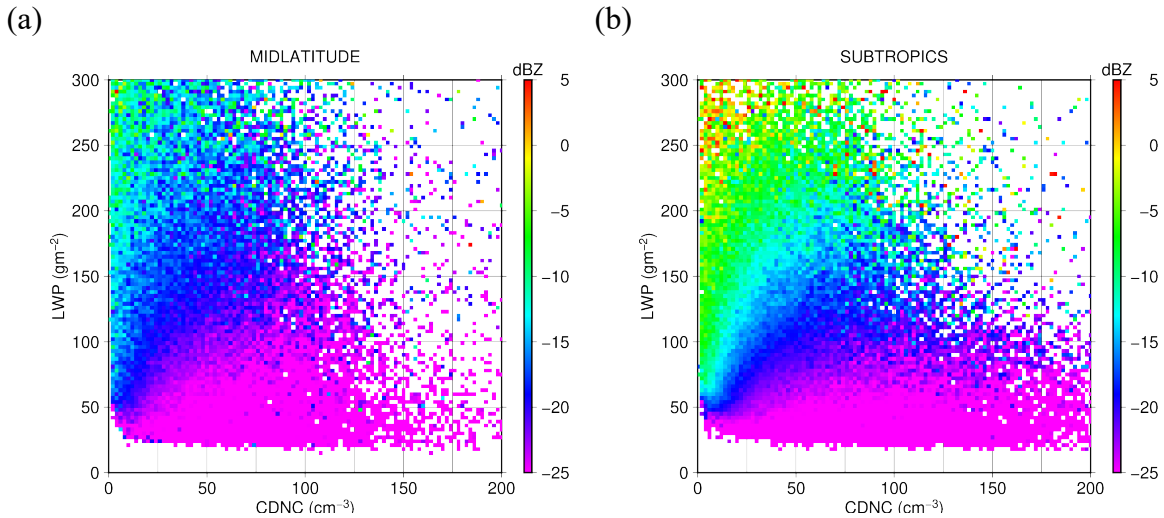

Figure 4.10 Same as Figure 4.8 but for cloud base radar reflectivity.

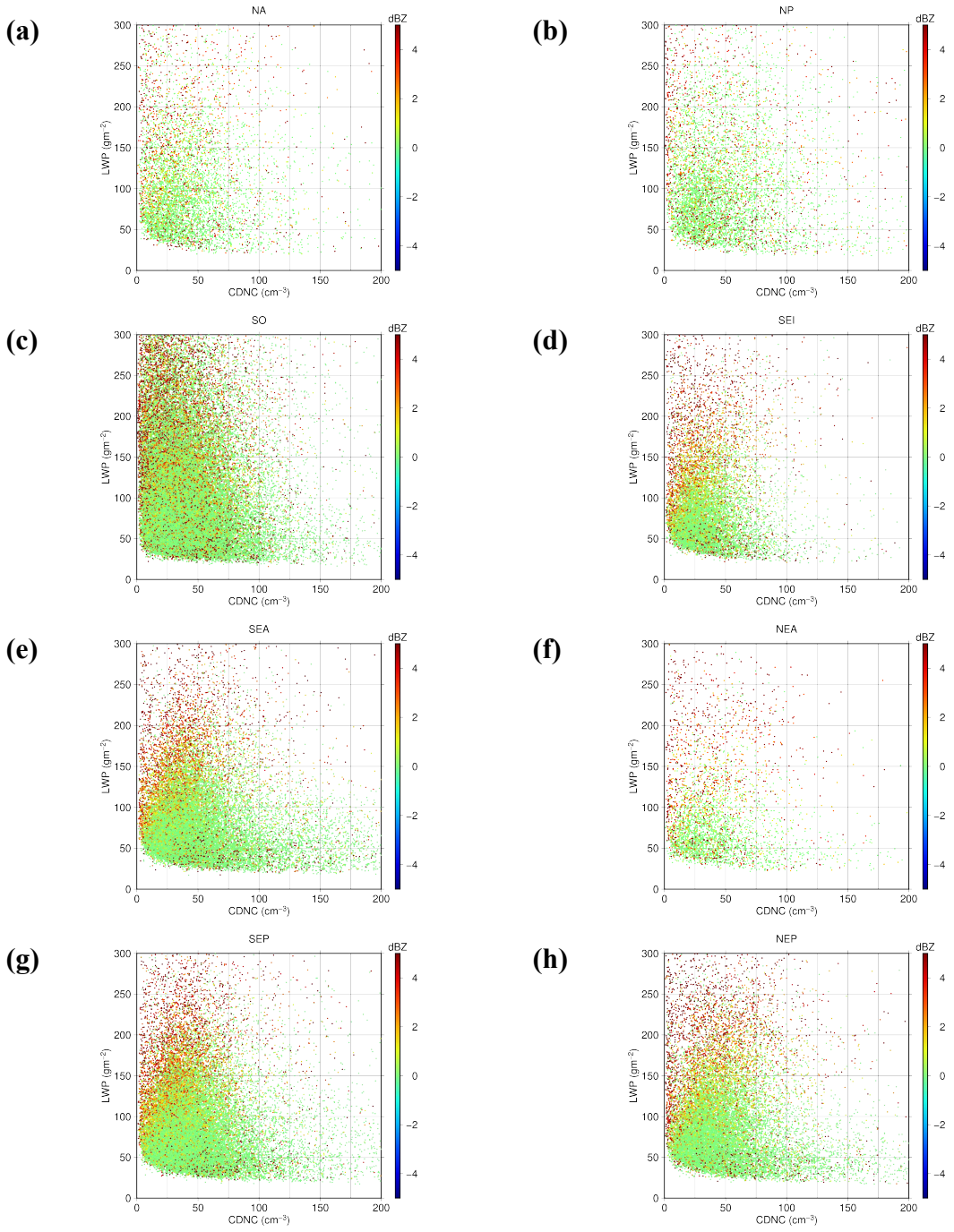

Figure 4.11 Scatterplot of increase in radar reflectivity(dBZ) from cloud top to base as a function of cloud droplet number concentration(CDNC)(cm^{-3}) and LWP(gm^{-2}) for (a) NA, (b) NP, (c) SO, (d) SEI, (e) SEA, (f) NEA, (g) SEP, (h)

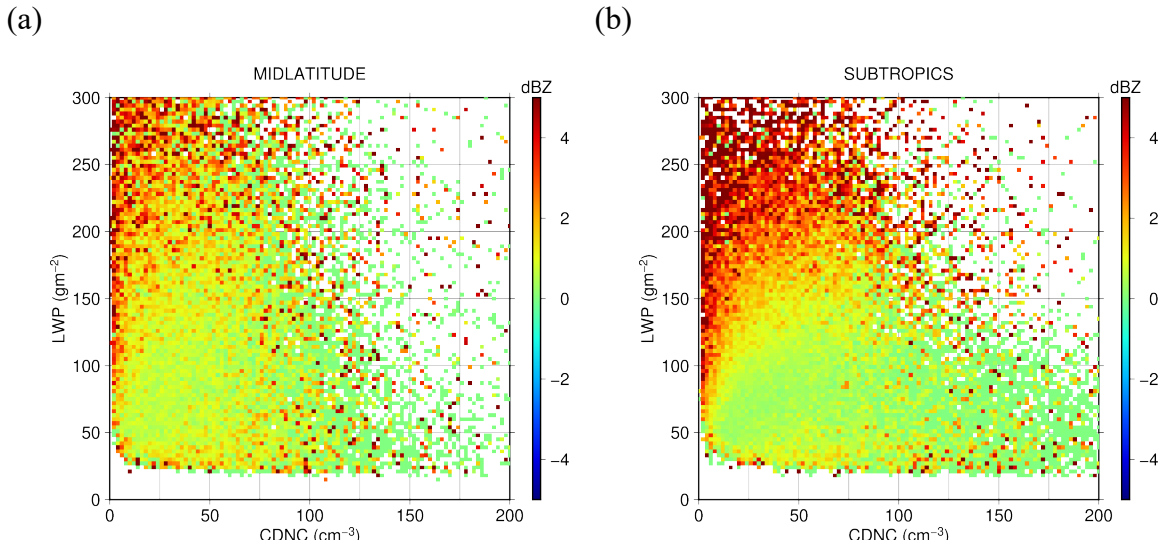

Figure 4.12 Mean increase in radar reflectivity(dBZ) from cloud top to base as a function of cloud droplet number concentration(CDBC)(cm^{-3}) and LWP(gm^{-2}) for (a) midlatitude and (b) subtropical region.

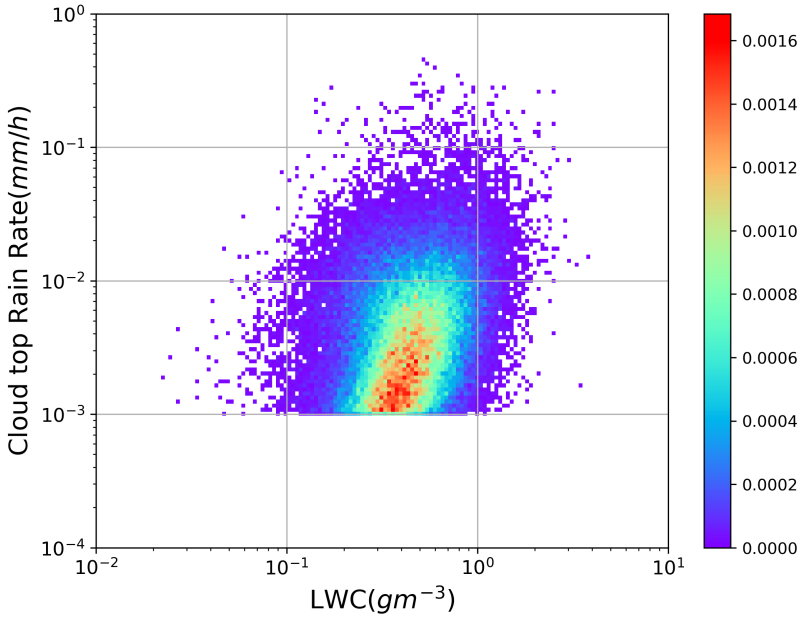

Figure 4.13 Probability distribution of cloud top rain rate(mm/h) as a function of cloud top LWC(gm^{-3}) for subtropical stratocumulus regions. (i.e., SEI, SEA, NEA, SEP, NEP).

(a) (b)

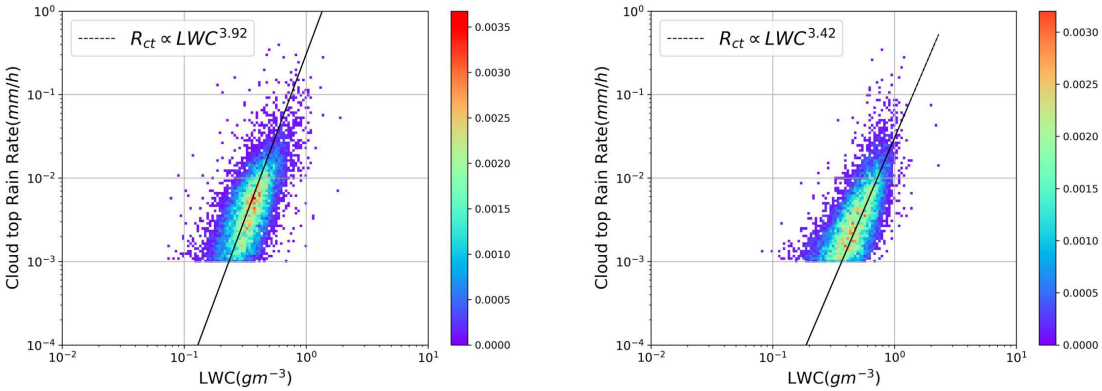

Figure 4.14 Same as Figure 4.13 but for clouds with cloud top cloud droplet number concentration of (a) $15 - 25\ cm^{-3}$ and (b) $35 - 45 cm^{-3}$.

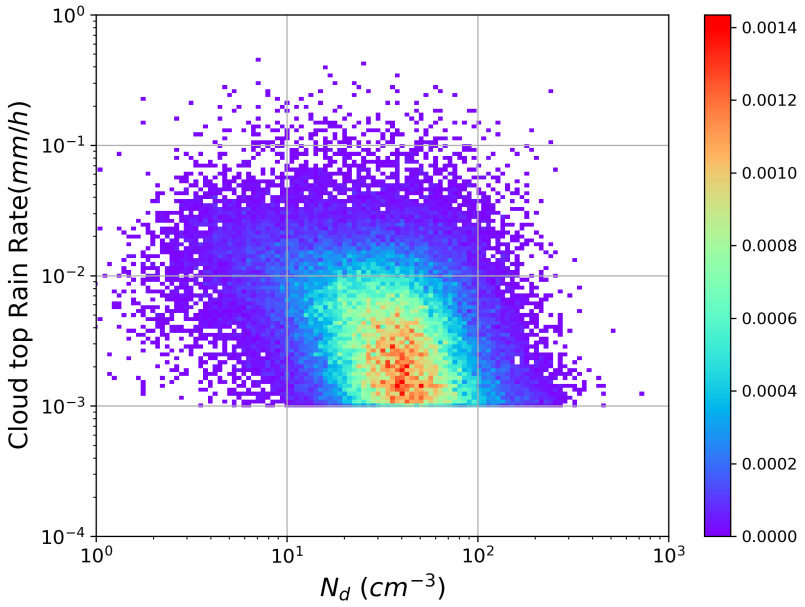

Figure 4.15 Probability distribution of cloud top rain rate (mm/h) as a function of cloud top cloud droplet number concentration(gm^{-3}) for subtropical stratocumulus regions. (i.e., SEI, SEA, NEA, SEP, NEP).

(a) (b)

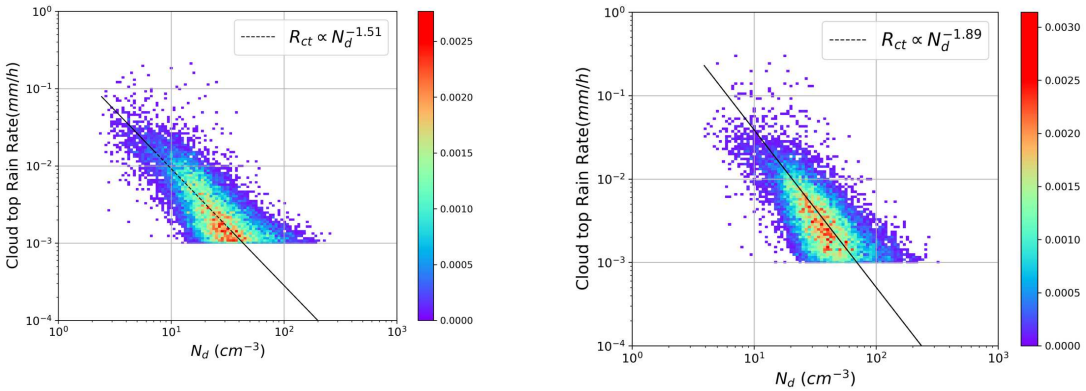

Figure 4.16 Same as Figure 4.15 but for clouds with cloud top LWC of (a) $0.25 - 0.35\ gm^{-3}$ and (b) $0.40 - 0.50 gm^{-3}$.

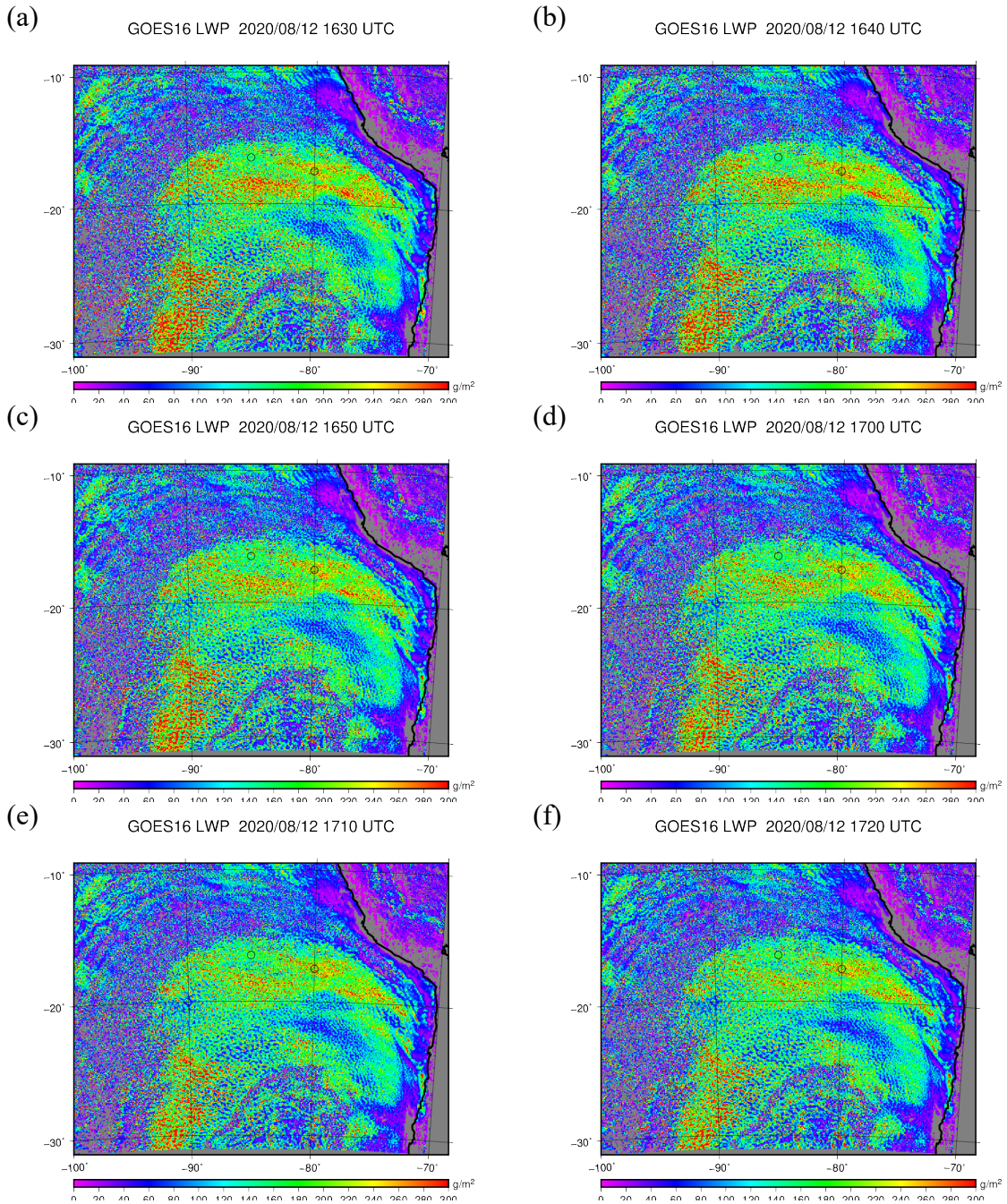

Figure 4.17 Example of time evolution of LWP(gm^{-2}) for stratocumulus clouds at SEP. Observation times are 2020/8/12 (a) 1630, (b) 1640, (c) 1650, (d) 1700, (e) 1710, (f) 1720 UTC.

Chapter 5

Conclusion

The overarching goal of this dissertation was to gain an understanding of the relationship between cloud top properties and precipitation processes, especially raindrop embryo production, in stratocumulus clouds with various cloud geometrical thicknesses and geographical locations. Cloud properties were retrieved using multi-sensor A-Train satellites observations from *CloudSat's* Cloud Profiling Radar (CPR), CALIPSO's Cloud-Aerosol Lidar with Orthogonal Polarization (CALIOP) and Aqua's Moderate Resolution Imaging Spectroradiometer (MODIS). The use of satellite observations made it possible to obtain statistically robust results, as well as to compare the many distinct regions presented in this study.

In Chapter 3, the relations between near cloud top properties (radar reflectivity, LWC and cloud droplet number concentration) and cloud geometrical thickness were investigated for subtropical stratocumulus clouds. The dependence of stratocumulus precipitation processes on cloud geometrical thickness, cloud top properties and environmental parameters was discussed based on their position on Z-LWC diagrams. The satellite observations show that cloud top LWC and effective radius increase as clouds becomes thicker. Base on the Z-LWC diagram, it was suggested that near cloud top raindrop embryo production (i.e. autoconversion) is enhanced for thicker clouds. These findings are consistent with the previous studies that thicker clouds have larger cloud droplets and thus produce more rain embryos. However, satellite observations also demonstrate that clouds become bimodal (drizzling and non-drizzling) as they transition from thick (i.e. geometrical thickness of 384-480m) to very thick clouds (i.e. geometrical thickness of 624-720m). Drizzling clouds have higher LWC and larger effective radius, whereas non-drizzling clouds have lower cloud top LWC and smaller effective radius.

The relations between cloud top reflectivity, LWC and cloud droplet number concentrations were found to be almost the same for all subtropical stratocumulus clouds regardless of their cloud geometrical thickness. The relations agree with the bulk model representations of autoconversion

and accretion processes that rain production rates increase with larger LWC and smaller cloud droplet number concentration . It was also found that the effective radius is a good predictor for cloud top radar reflectivity, which is similar to the findings of Rosenfeld et al. (2012) who demonstrated that column maximum rain rate increases with effective radius.

In warm clouds, the cloud base rain rate is the combined result of autoconversion and accretion. While the results showed that relative contribution of accretion to cloud base rain rate increases with greater LWP or higher geometrical thickness, it was found that cloud base radar reflectivity is mostly determined by cloud top radar reflectivity for subtropical stratocumulus clouds, irrespective of geometrical thickness.

In Chapter 4, the climatology of satellite-derived cloud top properties (radar reflectivity, LWC and cloud droplet number concentration) for 8 stratocumulus cloud regions were presented with a focus on the differences between subtropical and midlatitude regions. Responses of cloud top and base radar reflectivity to cloud top LWC, cloud droplet number concentration and LWP were also investigated and their implications for the bulk parameterization of precipitation processes in stratocumulus clouds were discussed.

As was found in the previous studies, distinct differences were also found in the climatology of cloud properties between subtropical and midlatitude stratocumulus clouds. While LWP tended to be larger for midlatitude clouds, cloud top LWC tended to be larger for subtropical stratocumulus clouds, which suggests that effective condensation rates were larger for subtropical stratocumulus clouds. Both cloud top and base radar reflectivity tended to be larger for subtropical stratocumulus clouds.

It was found that cloud top radar reflectivity could be parameterized with a globally applicable expression when parametrized as a function of cloud top LWC and cloud droplet number concentration, which is consistent with many bulk representations of autoconversion and accretion process. Cloud base radar reflectivity could also be represented by a globally applicable parameterization as a function of cloud top LWC and cloud droplet number concentration. In general, accretional growth is controlled by both the total cross-sectional area of rain drops and

LWP. By comparing spatial patterns of cloud top radar reflectivity (i.e. total cross-sectional area of rain drops) with the radar reflectivity increase from cloud top to bottom (i.e. accretional growth), it was found that accretional growth depended more on total cross-sectional area of rain drops and less on LWP in stratocumulus clouds.

Cloud top radar reflectivity was more (less) sensitive to changes in LWC and cloud droplet number concentration for cloud with stronger (weaker) cloud top radar reflectivity. This is consistent with the fact that collision-coalescence efficiency between liquid water droplets (of approximately 20 μm in diameter) increases non-linearly with droplet size (e.g. Hall 1980).

The results presented in this dissertation indicate that the autoconversion process can be represented with a globally uniform function of cloud top LWC and cloud droplet number concentration for all stratocumulus clouds regardless of their geolocation and geometrical thickness. It was also demonstrated that cloud top raindrop embryo generation rate is an important factor for determining the precipitation generation rate for stratocumulus clouds as a whole.

These conclusions can explain the findings of previous studies that cloud base rain rate depends on LWP (or cloud thickness) and geographical location of stratocumulus clouds. Cloud base rain rate is dependent on geometrical thickness because cloud top LWC increases as cloud become thicker. Subtropical stratocumulus clouds tend to have stronger precipitation rates at a given LWP compared to midlatitude clouds because the effective condensation rate of subtropical clouds is greater and so is the cloud top LWC. The results presented in this study also provide a benchmark that numerical weather models should reproduce. What is now left to be done is use these results to assess how well a numerical cloud model can reproduce the observations evaluated in this dissertation.

References

Ackerman, A. S., O. B. Toon, D. E. Stevens, and J. A. Coakley, 2003: Enhancement of cloud cover and suppression of nocturnal drizzle in stratocumulus polluted by haze. *Geophys. Res. Lett.*, **30**, 1381, doi: 10.1029/2002GL016634.

Albrecht, B. A., 1989: Aerosols, cloud microphysics, and fractional cloudiness. *Science*, **245**, 1227–1230.

Bennartz, R. and J. Rausch, 2017: Global and regional estimates of warm cloud droplet number concentration based on 13 years of AQUA-MODIS observations, *Atmos. Chem. Phys.*, **17**, 9815–9836, doi: 10.5194/acp-17-9815-2017.

Berry, E. X., and R. L. Reinhardt,1974: An analysis of cloud drop growth by collection: part II. Single initial distributions. *J. Atmos. Sci.*,**31**,1825–1831.

Brenguier, J. L., F. Burnet, and O. Geoffroy, 2011: Cloud optical thickness and liquid water path – does the *k* coefficient vary with droplet concentration?. *Atmos. Chem. Phys*., **11**, 9771–9786, doi: 10.5194/acp-11-9771-2011.

Comstock, K. K., R. Wood, S. E. Yuter, and C. S. Bretherton, 2004: The relationship between reflectivity and rain rate in and below drizzling stratocumulus. *Quart. J. Roy. Meteor. Soc.*, **130,** 2891–2918.

Eastman, R., R. Wood, and K. T. O, 2017: The subtropical stratocumulus-topped planetary boundary layer: A climatology and the Lagrangian evolution. *J. Atmos. Sci.*, **74**, 2633–2656, https://doi.org/10.1175/JAS-D-16-0336.1.

Grosvenor, D. P., and Coauthors, 2018: Remote sensing of droplet number concentration in warm clouds: A review of the current state of knowledge and perspectives. *Rev. Geophys.*, **56**, 409–453

Hall, W. D., 1980: A detailed microphysical model with a two-dimensional dynamic framework: Model description and preliminary results. *J. Atmos. Sci.*, **37 ,** 2486–2507.

Hu, Y., and Coauthors, 2007: Global statistics of liquid water content and effective number concentration of water clouds over ocean derived from combined CALIPSO and MODIS measurements, *Atmos. Chem. Phys.*, **7**, 3353–3359,doi:10.5194/acp-7-3353-2007.

Khain, A. P., , M. Pinsky, , L. Magariz, , O. Krasnov, , and H. W. J. Russchenberg, 2008: Combined observational and model investigations of the *Z*–LWC relationship in stratocumulus clouds. *J. Appl. Meteor. Climatol.*, **47**, 591–606.

Khairoutdinov, M., and Y. Kogan, 2000: A new cloud physics parameterization in a large-eddy simulation model of marine stratocumulus. *Monthly Weather Review*, **128**, 229– 243.

Klein, S. A., and D. L. Hartmann, 1993: The seasonal cycle of low stratiform clouds. *J. Climate*, **6**, 1587–1606.

Klein, S. A., , D. L. Hartmann, , and J. R. Norris, 1995: On the relationships among low-cloud structure, sea surface temperature, and atmospheric circulation in the summertime northeast Pacific. *J. Clim.*, **8**, 1140–1155.

Leon, D. C., Z. Wang, and D. Liu, 2008: Climatology of drizzle in marine boundary layer clouds based on 1 year of data from CloudSat and Cloud-Aerosol Lidar and Infrared Pathfinder Satellite Observations (CALIPSO). *J. Geophys. Res.*, **113**, D00A14, doi: 10.1029/2008JD009835.

Liebe, H. J., T. Manabe and G.A. Hufford, 1989: Millimeter-wave attenuation and delay rates due to fog/cloud conditions. I*EEE Trans. Antenn. Prop.*, **37**, 1617-1623.

Liu, Y., and P. H. Daum, 2004: On the parameterization of the autoconversion process. Part I: Analytical formulation of the Kessler-type parameterizations. *J. Atmos. Sci.*, **61**, 1539–1548.

Long, A. B., 1974: Solutions to the droplet collection equation for polynomial kernels. *J. Atmos. Sci.*, **31**, 1040–1052.

Lu, M. -L., W. C. Conant, H. H. Jonsson, V. Varutbangkul, R. C. Flagan, and J. H. Seinfeld, 2007: The marine stratus/stratocumulus experiment(MASE): Aerosol-cloud relationships in marine stratocumulus, *J. Geophys. Res*., **112**, D10209, doi:10.1029/2006JD007985.

Lu, M. L., A. Sorooshian, H. H. Jonsson, G. Feingold, R. C. Flagan, and J. H. Seinfeld, 2009 Marine stratocumulus aerosol cloud relationships in the MASE-II experiment: Precipitation susceptibility in eastern Pacific marine stratocumulus, *J. Geophys. Res*., **114**, D24203, doi:10.1029/2009JD012774.

Mace, G. G., and Q. Zhang, 2014: The CloudSat radar-lidar geometrical profile product (RL-GeoProf): Updates, improvements, and selected results. *J. Geophys. Res. Atmos.*, **119**, doi: 10.1002/ 2013JD021374.

Mann, J. A. L., J. C. Chiu, R. J. Hogan, E. J.O'Connor, T. S. L'Ecuyer, T. H. M. Stein, and A. Jefferson, 2014: Aerosol impacts on drizzle properties in warm clouds from ARM Mobile Facility maritime and continental deployments, *J. Geophys. Res. Atmos.*, **119**, 4136– 4148, doi:10.1002/2013JD021339

Marchand, R., G.G. Mace, T. Ackerman, and G. Stephens, 2008: Hydrometeor Detection Using Cloudsat—An Earth-Orbiting 94-GHz Cloud Radar. *J. Atmos. Oceanic Technol.*, **25**, 519–533.

Miller, D. J., Z. Zhang, A. S. Ackerman, S. Platnick, and B. A. Baum, 2016: The impact of cloud vertical profile on liquid water path retrieval based on the bispectral method: A theoretical study based on large-eddy simulations of shallow marine boundary layer clouds, *J. Geophys. Res. Atmos.*, **121,** 4122– 4141, doi:10.1002/2015JD024322.

Muhlbauer, A., I. L. McCoy, and R. Wood, 2014: Climatology of stratocumulus cloud morphologies: microphysical properties and radiative effects, *Atmos. Chem. Phys.*, **14**, 6695–6716, doi: 10.5194/acp-14-6695-2014.

Nicholls, S. and J. Leighton, 1986: An observational study of the structure of stratiform cloud sheets: Part I. Structure. *Quart. J. Roy. Meteor. Soc.*, **112**, 431–460.

Norris J.R. and S. A. Klein, 2000: Low cloud type over the ocean from surface observations. Part III: relationship to vertical motion and the regional surface synoptic environment. *J. Clim*. **13**, 245–256.

Parkinson, C.L., 2003: Aqua: An earth-observing satellite mission to examine water and other climate variables. *IEEE Trans. Geosci. Remote Sens.,* **41(2)**, 173-183.

Platnick, S., and Coauthors, 2017: The MODIS Cloud Optical and Microphysical Products: Collection 6 Updates and Examples From Terra and Aqua. *IEEE Trans. Geosci. Remote Sens.*, **55(1)**, 502-525.

Rogers, R. R., and M. K. Yau, 1989: *A Short Course in Cloud Physics.* 3rd ed. Pergamon Press, 304 pp.

Rosenfeld, D., H. L. Wang, and P. J. Rasch, 2012: The roles of cloud drop effective radius and *LWP* in determining rain properties in marine stratocumulus. *Geophys. Res. Lett.*, **39**, L13801, doi:10.1029/2012GL052028.

Rossow, W.B., and R.A. Schiffer, 1991: ISCCP Cloud Data Products. *Bull. Amer. Meteor. Soc.*, **71**, 2-20.

Slingo, A., 1990: Sensitivity of the Earth's radiation budget to changes in low clouds. *Nature*, **343,** 49–51.

Stephens, G.L., D.G. Vane, R.J. Boain, G.G. Mace, K. Sassen, Z. Wang, A.J. Illingworth, E.J. O'Connor, W.B. Rossow, S.L. Durden, S.D. Miller, R.T. Austin, A. Benedetti, C. Mitrescu, and CloudSat Science Team, 2002: The CloudSat mission and the A-Train: A new dimension of space-based observations of clouds and precipitation. *Bull. Amer. Meteorol. Soc*., **83**, 1771-1790, doi:10.1175/BAMS-83-12-1771.

Twomey, S., 1959: The supersaturation in natural clouds and the variation of cloud droplet concentration. *Geofis. Pura Appl.,* **43,** 243–249.

vanZanten, M. C., B. Stevens, G. Vali, and D. Lenschow, 2005: Observations of drizzle in nocturnal marine stratocumulus. *J. Atmos. Sci.*, **62**, 88–106.

Wang, H., P. J. Rasch, and G. Feingold, 2011: Manipulating marine stratocumulus cloud amount and albedo: a process-modelling study of aerosol-cloud-precipitation interactions in response to injection of cloud condensation nuclei, *Atmos. Chem. Phys.*, **11**, 4237–4249, doi: 10.5194/acp-11-4237-2011.

Winker D. M. and Coauthors., 2009: Overview of the CALIPSO mission and CALIOP data processing algorithms. *J. Atmos. Ocean. Technol.*, **26**, 2310-2323.

Wood, R., 2005a: Drizzle in stratiform boundary layer clouds. PartI: Vertical and horizontal structure. *J. Atmos. Sci.*, **62**, 3011–3033.

Wood, R., 2005b: Drizzle in stratiform boundary layer clouds. PartII: Microphysics aspects. *J. Atmos. Sci.*, **62**, 3034–3050, doi: 10.1175/JAS3530.1.

Wood, R, 2012: Stratocumulus clouds. *Mon. Wea. Rev.*, **140**, 2373–2423.

Wood, R., and C. S. Bretherton, 2004: Boundary layer depth, entrainment, and decoupling in the cloud-capped subtropical and tropical marine boundary layer. *J. Clim.*, **17 ,** 3576–3588.

Wood, R. and Coauthors., 2011: The VAMOS Ocean-Cloud-Atmosphere-Land Study Regional Experiment (VOCALS-REX): Goals, platforms, and field operations, *Atmos. Chem. Phys*., **11**,

627–654, doi:10.5194/acp-11-627-2011.